FILE COPY

J. GREGORY

Rev 21

UNDERWATER SOLID STATE CAMERA

(SATODA PROGRAM)

ANDREW G LYN.

OCEAN ELECTRONIC APPLICATIONS, INC
50 West Mashta Drive
Key Biscayne, Florida
33149

TABLE OF CONTENTS

SADOTA "EYE"

The SADOTA "EYE" is an underwater solid state camera. Its primary features are:

(a) Solid State Image Sensor
(b) Low Power Consumation
(c) Low Light Level Sensitivity
(d) Computer Interface

The heart of the camera is a Reticon RA100X100 solid state image sensor. There are 10,000 light sensitive elements arranged in a 100X100 matrix on the chip. This results in a high resolution image.

The sensor is positioned at the focal point of a f1.2;7-45MM power zoom lens, (focusing five feet to infinity).

By using a majority of CMOS components, a low power drain is realized. This makes the unit suitable for portable battery operation.

The aperture is mode selectable from manual, fixed to automatic. In the automatic mode, optimum exposure level is maintained even if the scene intensity varies severely from dark to light. The sensor uses a diode array and bucket-brigade registers to sense and transfer charges due to the integrated light level. Therefore, slowing or speeding up the sample rate has an effect similar to the opening and closing of the aperture.

Except for the analog video output, all of the signals are digital in nature. This allows easy adaption to computerized control. Such a system could digitize and store the video information for later dissemination via electrical or acoustical means.

The camera is enclosed in a corrosion resistant underwater housing capable of withstanding pressures to depths of 1000 feet.

Camera Optics.

The camera optics consist of a Bell and Howell f1.2, 7-45 mm focal length zoom lens, a supplementary lens and a spherical glass port.

The spherical glass port was chosen because it exhibits excellent hydrostatic pressure resistance and less aberration as compared to a plane port. Other advantages are: (a) the same field of view of the camera lens if no vignetting is present; and (b) no change in the effective focal length of the camera.

Port Specifications:
- Inner Radius of Curvature: 3.5 inches
- Thickness: 0.50 inches
- Material: Crown Glass
- Surface Quality: 80-50
- Sized to produce a 60 angle with the center of curvature.

The supplementary lens is used to correct the diverging lens effect caused by the spherical dome in water. The camera lens and supplementary lens set are positioned three and one half inches from the center of the dome window.

Supplementary Lens Specs: +3 (2.8) Diopters

For maximum field of view and resolution, a zoom lens is necessary. The Bell and Howell lens was designed for a Super-8 movie format which is similar in dinension to the active area of the Reticon RA100X100 Integrated Circuit. As a result of this and also because of a cost/performance trade off, this lens system was adopted.

Construction

The SADOTA "EYE" solid state camera consists of four interconnecting boards. They are:

(a) Sensor Board
(b) Timing Board
(c) Aperture/Zoom Board
(d) Control Board

The sensor board provides electrical connections to the Reticon solid state image sensor array (RA100X100). On the periphery of the board are multiple-pin sockets which provide the common mechanical and electrical connection to the remaining three boards. The board is also used to position the RA100X100 at the focal point of the lens system.

The timing board generates the clocks 0x1, 0x2, 0y1, 0y2 and the functions of LR and LT. These are synthesized from a single variable oscillator. Each line of picture information is transferred in parallel to an on chip analog shift register. From the register, the information is moved sequentially to the output under control of the 0x clocks. Information from the next line is then accessed under control of the 0y clocks and transferred to the x registers, etc.

The relationship between the clocks and the functions of LR and LT can be found in Figure 1(b). This is quite critical to successful operation of the camera. The FC (or Frame Control) is used to provide a single frame, to provide continuous frames or to disable the PxCx (Pixel Clocks). See Figure 1(a). This, in turn, disables the video.

The aperture/zoom board consists of the control of aperture and zoom, and combines the video with sync signals to form a composite video. The aperture and zoom controls are dependent on the settings of a 2 bit binary word and a pulse input (Po).

There are four aperture modes: Automatic, Fixed, Closed and Open. In the automatic mode, the aperture adjusts to an optimum preset level regardless of changes in light intensity or clock speed (2X clock). By selecting aperture mode open or closed and pulsing the input, any f stop can be chosen. This value can be held by selecting the fixed mode.

Combined video is obtained by taking the buffered, interlaced video output of the RA100X100 I.C. and combining it with the EOF (End of Frame Strobe) and the LT (Line Transfer) outputs. This gives a negative, vertical sync and video voltages of 2V P'P,. Video black is OV; video white is 4V at sensor saturation. See Figure 1(c)

The control board houses the 10 turn potentiometers that control:

ODD/EVEN Balance
BIAS Adjust
V BUFF (Blooming Adjust)
VBB " "
LR/LT Adjust

These set the DC Bias levels for the RA100X100 I.C. See Figure 14.

Board Alignment

Initial Board Setup

(1) Adjust VIDEO BALANCE and ODD/EVEN BALANCE pots to the center of their ranges.
(2) Adjust V BUFF potentiometer to produce 12.5 volts at the RA100X100 Pin 15.
(3) Adjust BIAS ADJUST to produce 4.5 volts at the RA100X100 Pin 6.
(4) Adjust VBB potentiometer to give 12 volts at the RA100X100 Pin 19.
(5) Adjust LR CONTROL fully clockwise.
(6) Connect a pulse generator to (2X clock) input, set frequency at 500 KHz.

Final Board Setup

(1) Cover most of the array window with black tape except for a narrow opening from Pin 8 to Pin 17.

Illuminate the RA100X100.

Connect a scope probe to the ODD video output, RA100X100 Pin 12.

Sync the scope to LT. (Timing Board, IC 4013-A Pin 1).

Pass your hand between the light source and the RA100X100 observing the reaction of the video output. The odd video output should resemble Figure 3(a).

Adjust BIAS ADJUST until the last three elements are first equal in amplitude. See Figure 3(b).

(2) Move the scope probe to the VIDEO BALANCE pot, (TPV), Figure 6. Sync the scope on EOF.

Completely darken the RA100X100. Adjust ODD/EVEN BALANCE until the odd/even pattern is at a minimum. See Figure 2(b).

Allow light to fall on the RA100X100. Adjust VIDEO BALANCE until the odd/even pattern on the scope is at a minimum. See Figure 2(a).

(3) Completely darken the RA100X100. Turn LR CONTROL counter-clockwise until noise appears. Then adjust clockwise until noise disappears. Continue clockwise 1/4 turn.

(4) Cover the RA100X100 with a piece of black tape that has a very small hole in the middle of the array.

Increase the illumination intensity enough to cause severe blooming. See Figure 5(a).

Blooming is defined here as a significant response from darkened pixels when nearly illuminated pixels are greatly over saturated by excessive light.

Adjust VBUFF to minimise the blooming effect as in Figure 5(b).

Adjust VBB to be between 11 or 12 VDC. The output of the saturated video line will clip when the dc voltage level of VBB is too high. Lower VBB until there is no further improvement in the clipping.

Camera Specifications

Camera Power Supply	Typ.	+15VDC
	Max.	17V
	Min.	11V
Current Drain (Dependent on Frequency of 2X clock)	Max.=87mA @ 2MHZ Typ.=65mA @ 40KHz-1MHz	
Dark Rate (Low Light Level)	Min. =	40KHz
	Max. =	70KHz
Dark Rate (Bright Sunlight)	Min. =	76KHz
	Max. =	2MHz (*)
Dynamic Range	100:1	
Zoom Motor Drive	Typ. =	30mA

Lens: f 1.2 7-45mm Zoom
focusing 1.5m (5 feet to infinity), Macro Lens

Sensor: See RA100X100 data sheet.

(*) Limited by display interface, SVD Board.

Circuit Description - Aperture/Zoom Board

Combined Video

The odd and even video from the RA100X100 I.C. are combined by the VIDEO BALANCE Potentiometer. By adjusting this control the odd/even variation can be balanced out to give fully interlaced video. This is then fed into the input of buffer amp I.C. 301-A. The biasing network on pin 3 of this device gives peak sampling of the odd video signal which is used to produce the D.C. video level at the output of the buffer amp. The resultant output, (direct video), is a 2V d.c. level with 2V P-P video. The direct video across the 2K resistor RV, is switched by transistor Q1 to provide zero voltage level sync signals.

The resultant video signal is called the composite video. EOF (End of Frame) and LT (Line Transfer) are combined to produce the sync timing.

Aperture Control

The direct video also goes to integrator amp. I.C. 301-B. The output (TP1) of I.C. 301-B drives the window-comparator pair of 358A. Upper and lower trip points are 12.04V (Max), 10.95V (Min). The output of the 358A's are across two 10K resistor dividers. This produces 1/2VCC whenever TPI is within the maximum and minimum limits and, 0 Vots or VCC otherwise. This output is selected by I.C. 4051 (digitally controlled analog switch) and depending on a 3 bit code (See Table I), will be passed on to a second comparator pair 358B. These act as the power-driver for aperture mechanism and will open or close the aperture. If the video signal is within the optimum range of the 358A, then the aperture will remain fixed at that particular f stop. But an increase or decrease of scene intensity will cause a corresponding change of the integrator output (TPI), causing the aperture to open or close to try and maintain its optimum level. This results in automated aperture control. See Aperture/Zoom Board Schematic and Block Diagram, Figures 6 and 7.

Zoom Control

The comparator pair formed by I.C. LM 377 are biased so that there is a "window" voltage, within which input changes produce no effect on the output.

The I.C. 4051-B is used to switch the input of I.C. LM 377 outside this "window" producing the drive to the Zoom Motor. See Figure 6.

TABLE I

Po (MSB)	S2	S1 (LSB)	APERTURE	ZOOM
0	0	0	Automatic	----
0	0	1	Fixed	----
0	1	0	----	----
0	1	1	----	----
1	0	0	Closed	----
1	0	1	Open	----
1	1	0	----	In
1	1	1	----	Out

Circuit Description-Timing Board

A positve going transition on the FC line starts the frame. If FC line is held at logic one, the frame repeats, if it is held low, only one frame is outputted.

The FC control consist of 4013-B1, 4011-A1, A2, A3. See Figure 10.

I.C. 4017-A,B. forms the X pixel counter. Since there are 10,000 light sensitive elements arranged in a 100X100 matrix, the counter has to count 100 lines per field. After every 100th line, LT (Line Transfer) is outputted. LT clocks a flip-flop (4013-B2) which provides the 0y, and 0y2 complementary clock.

0x2 is derived by clocking 4013-A2 by the 2X clock.

As soon as LT goes high, 4017-C is enabled, allowing Q3 to go high. This resets LT after the third count of the 2X clock to provide the proper pulse width.

LT ANDed with 0x2 produce Ox and LR.

SVD BOARD

The SVD Board is the SADOTA "EYE" camera to oscilloscope interface. It enables the user to observe video images using the X, Y, and Z axis of an oscilloscope without interfacing to a computer. The board contains a sync separator which is used in conjunction with counters and D/A,s to generate horizontal and vertical scans.

The modulation for the Z axis is produced by amplifing and level shifting the combined video.

Two push buttons produce the zoom in/out effect. A 4 bit dip switch provide the codes necessary to select the different aperture modes as well as enabling the camera for continuous or single frame operation, (FC control). There is a variable oscillator which drives the 2X clock input of the camera.

The modulation level control should be adjusted for best picture contrast depending on the type oscilloscope used.

Circuit Description SVD Board

Transistors Q1, Q2 and counter I.C. 4024-A separate the sync signals, H sync and V sync from the combined video. I.C. 4024-A produces a count of the H sync which is applied to the clock input. The counter is reset by the V sync.

This count is then applied to the input of the Digital and Analog converter I.C. MC1408-A. The resulting analog output, a negative going ramp function is coupled to the Y axis of the scope. I.C. 4024-B and Mc 1408-B similarly produces the X axis scan.

The combined video is also amplified X 10 by I.C. 353 and coupled to the Z axis of the scope. This modulates the trace, and coupled with the X and Y scans, produce a video image.

I.C. 4046 is a phase locked loop opearting as a VCO (Voltage Controlled Oscillator). The VCO output is buffered by an I.C. 4069 inverter. This drives the 2X clock of the camera. Potentiometer RF varies the frequency from OHz to 1.5MHz. See Figures 8 and 9.

Camera Operation Using SVD Board

Place the SADOTA "EYE" on a suitable supporting base.

Connect the 9 Pin Seacon cable to the keyed socket on the back of the camera.

Apply +15VDC and ground to the power cables of the SVD board. (See SVD Board for Labeling.)

Connect H sync to the X input, V sync to the Y input and Video to the Z input of the oscilloscope. See Figure 13.

Set S1,S2,P0 of the dip switch to Logic "0".

Set 2X clock rate to approximately 400 - 500 KHz.

Set FC. of the dip switch to Logic "1".

Adjust the Volts/Division control to 20mV/Div.

With the scope on, adjust the brightness control until the square formed by the X,Y scan is visible. Use the Volts/Divison Variable adjustment to precisely control the size of the square.

Center the X,Y scan by adjusting the horizontal and vertical scope controls.

Set the camera lens focus for 10' distance.

Place an object 10' distance from the front of the lens.

Illuminate the object to about average brightness.

Press the ZOOM OUT control on the SVD board.

The object should be visible on the scope.

Press the ZOOM IN control and get a close up view of the object.

Adjust the scope Focus and Brightness control to optimise the video image.

In the auto-mode, S1,S2,P0 set at Logic "0", varying the intensity of the scene should not cause an appreciable change in picture quality.

However, for extreme low light levels the 2X clock can be slowed down to increase the sensitivity and visa versa for high light levels.

Depending on the design of the scope's Z axis input, the video modulation level can be increased or decreased by the VIDEO LEVEL Potentiometer on the SVD Board.

For manual operation of the camera aperture, see Figure 1.

Pulsing the Po line with S1,S2 in the closed or open mode, can precisely set the f stop. Setting P0,S1,S2 to fixed mode will then store this setting.

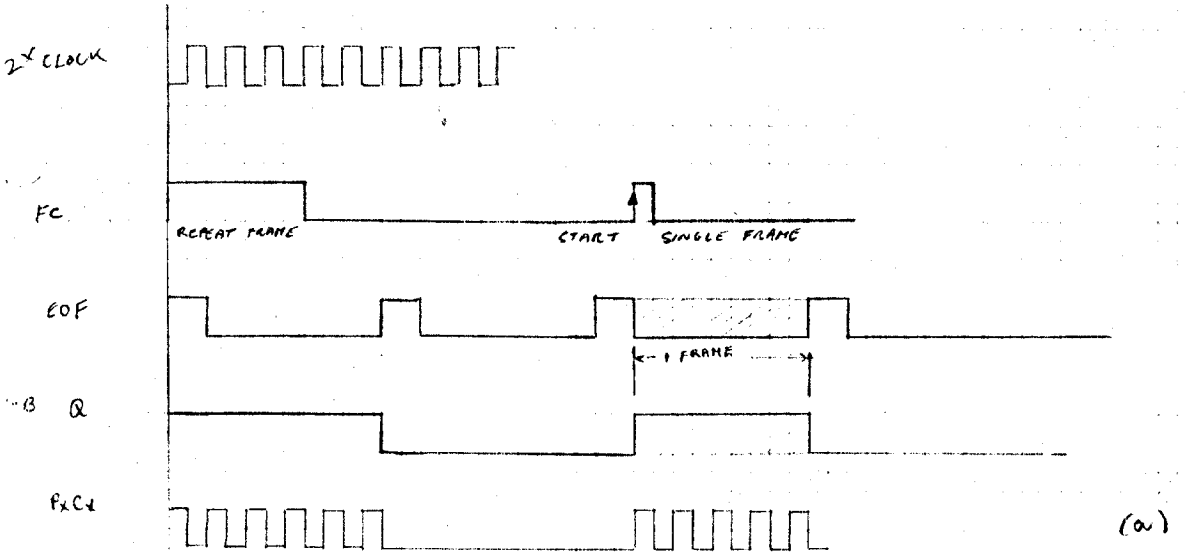
2X CLOCK
FC
REPEAT FRAME
START
SINGLE FRAME
EOF
1 FRAME
Q
FxCL

(a)

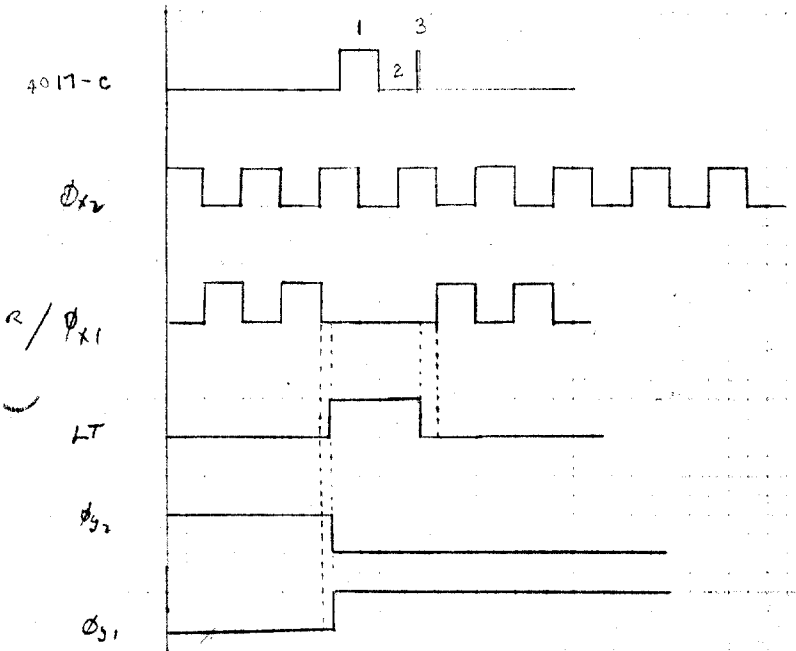
1
3
2
4017-C
ϕ_{x2}
R / ϕ_{x1}
LT
ϕ_{y2}
ϕ_{y1}

(b)

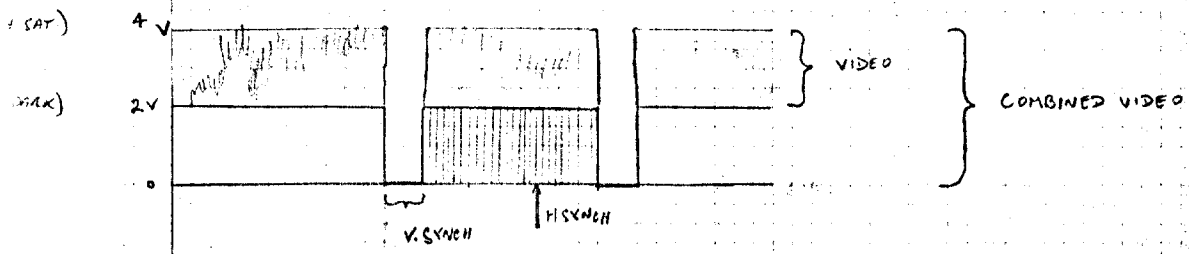
4 V
2V
0
V. SYNCH
H SYNCH
VIDEO
COMBINED VIDEO

(c)

fig. 1

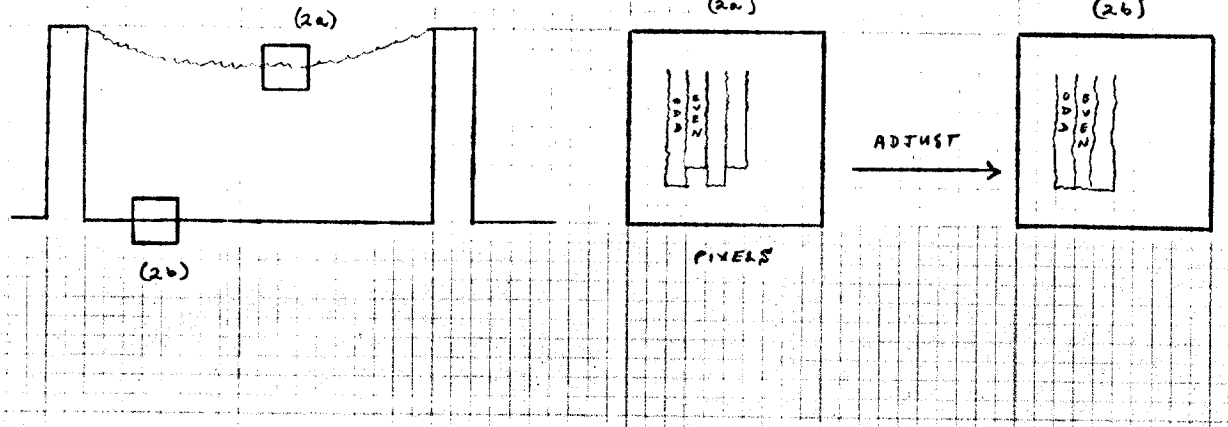

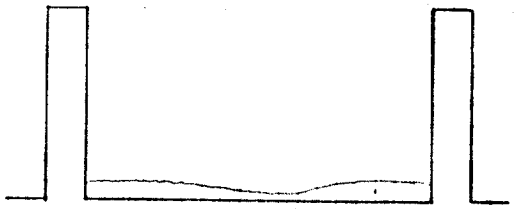

VIDEO SATURATION

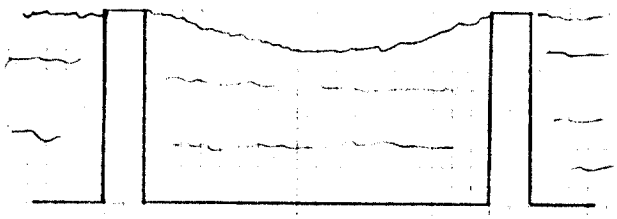

FIG 5(a)

BLOOMING ADJUSTMENT OFF

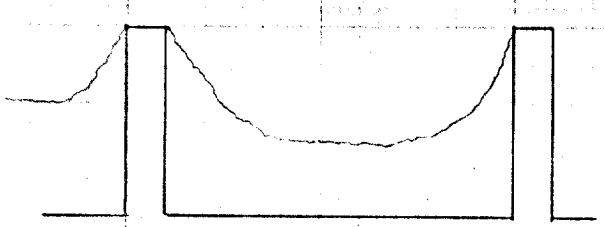

FIG. 5(b)

BLOOMING ADJUSTMENT O.K.

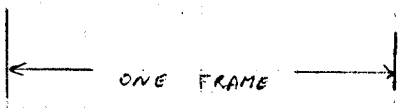

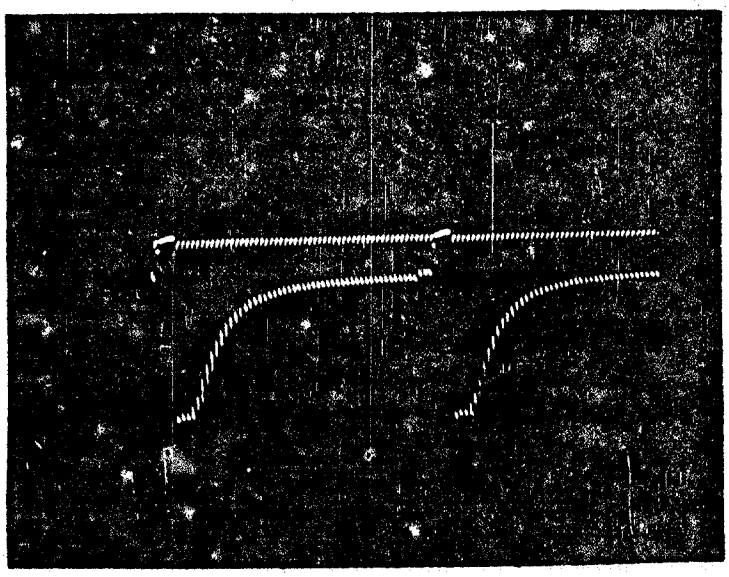

FIG 3(a)

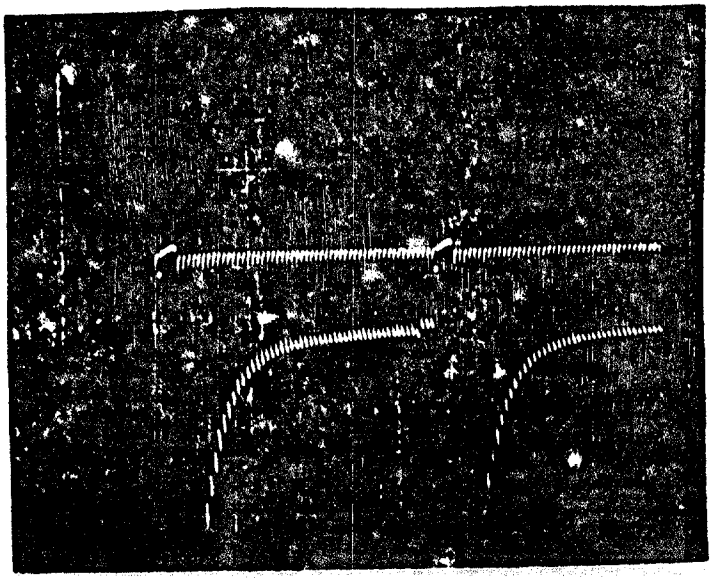

FIG 3(b)

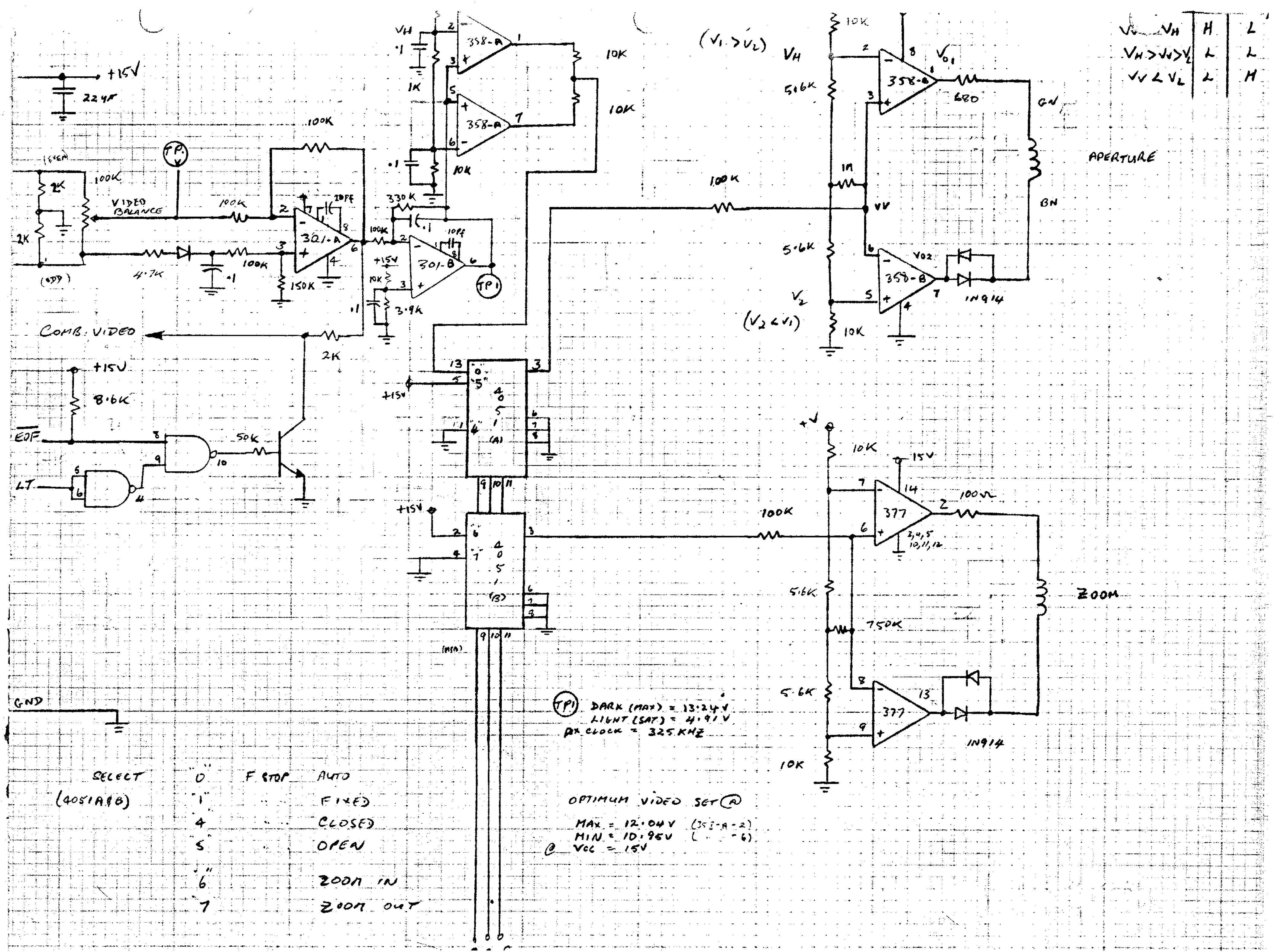

+15V
22µF
VIDEO BALANCE
TP V
100K
2K
301-A
301-B
TP1
358-A
358-B
VH
V1 > V2
V2 < V1
V01
V02
VV
680
GN
BN
APERTURE
1N914
COMB. VIDEO
8.6K
EOF
LT
50K
4051 (A)
4051 (B)
377
100Ω
750K
ZOOM
GND
VV > VH | H | L
VH > VV > VL | L | L
VV < VL | L | H
TP1 DARK (MAX) = 13.24V
LIGHT (SAT) = 4.91V
PX CLOCK = 325 KHZ
SELECT (4051A&B)
"0" F STOP AUTO
"1" FIXED
"4" CLOSED
"5" OPEN
"6" ZOOM IN
"7" ZOOM OUT
OPTIMUM VIDEO SET @
MAX = 12.04V (358-A-2)
MIN = 10.96V (-6)
@ VCC = 15V

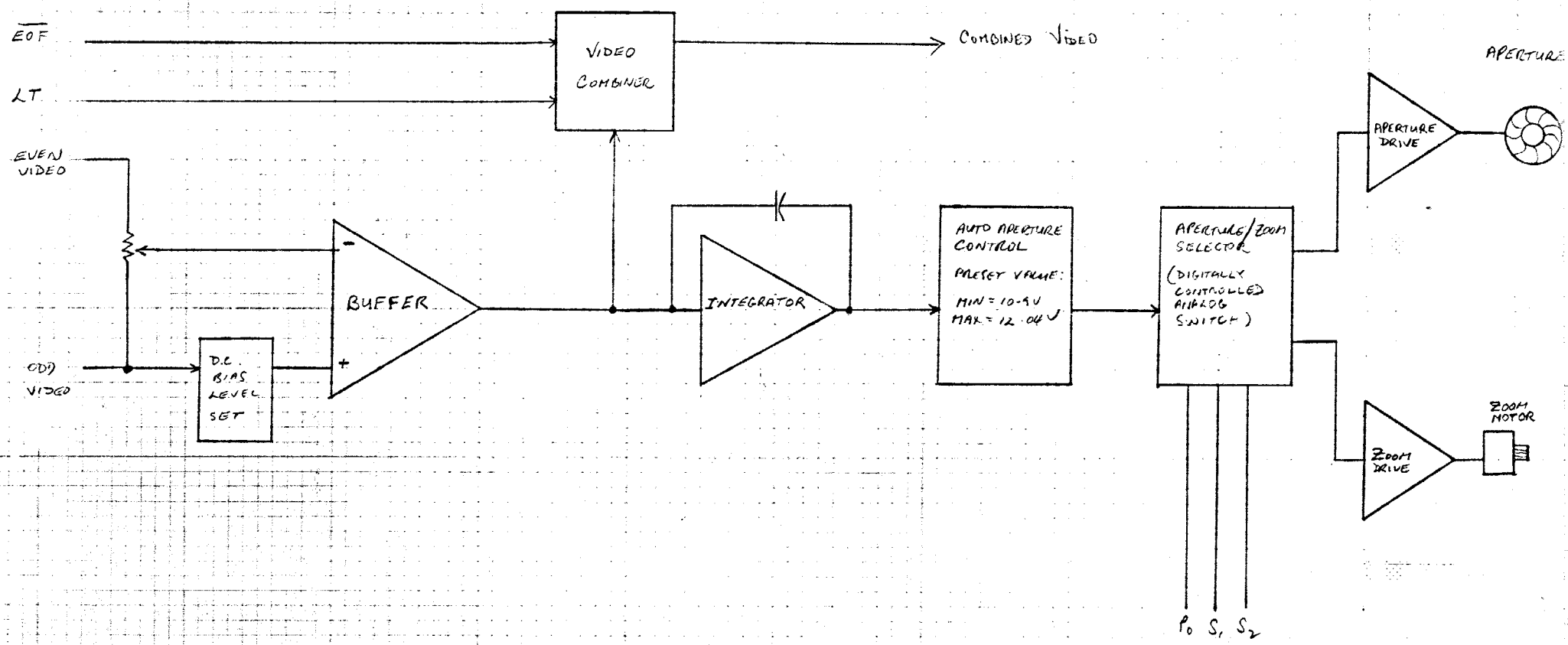

APERTURE / ZOOM (BLOCK DIAGRAM)

FIG. 7

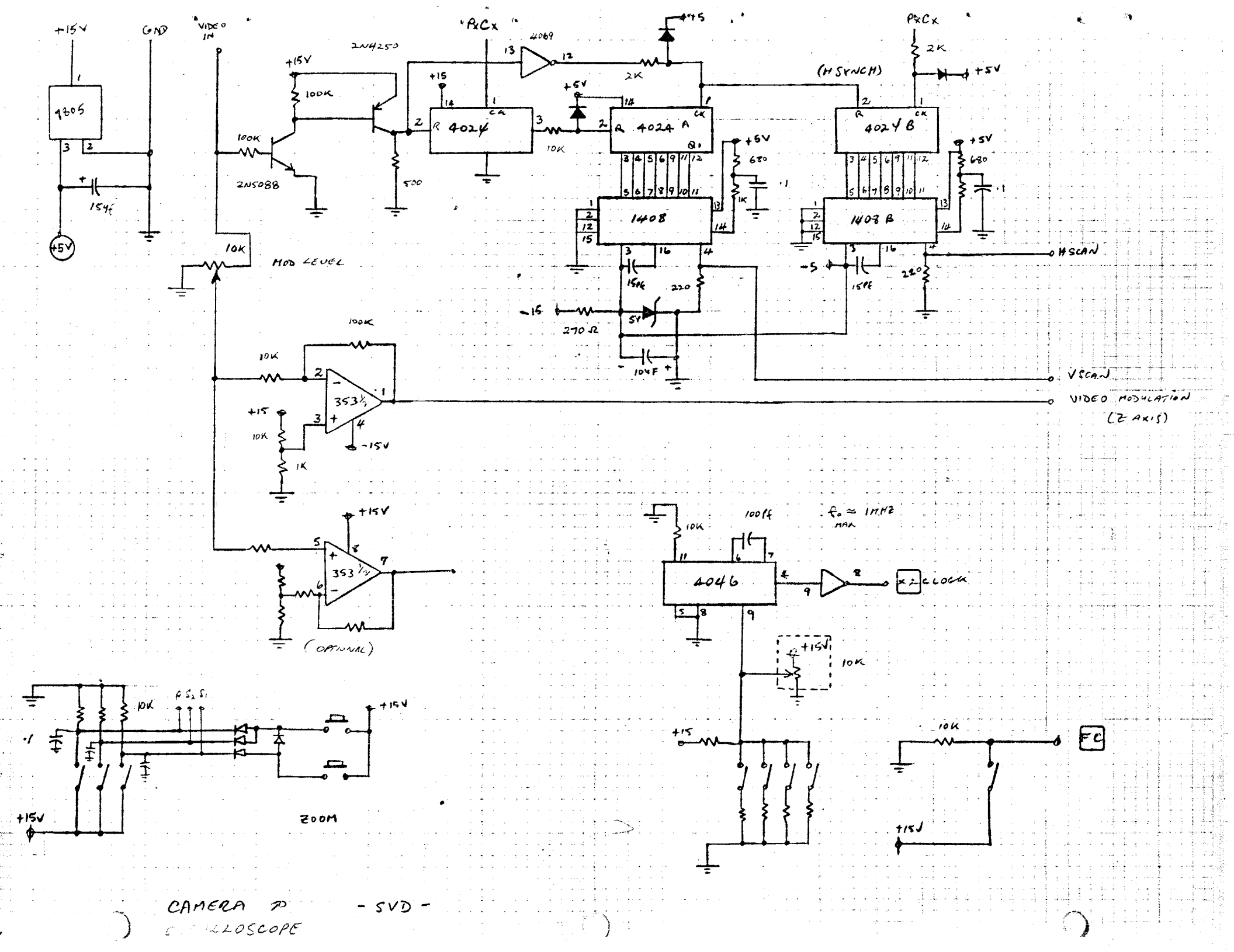

CAMERA ⇒ OSCILLOSCOPE

- SVD -

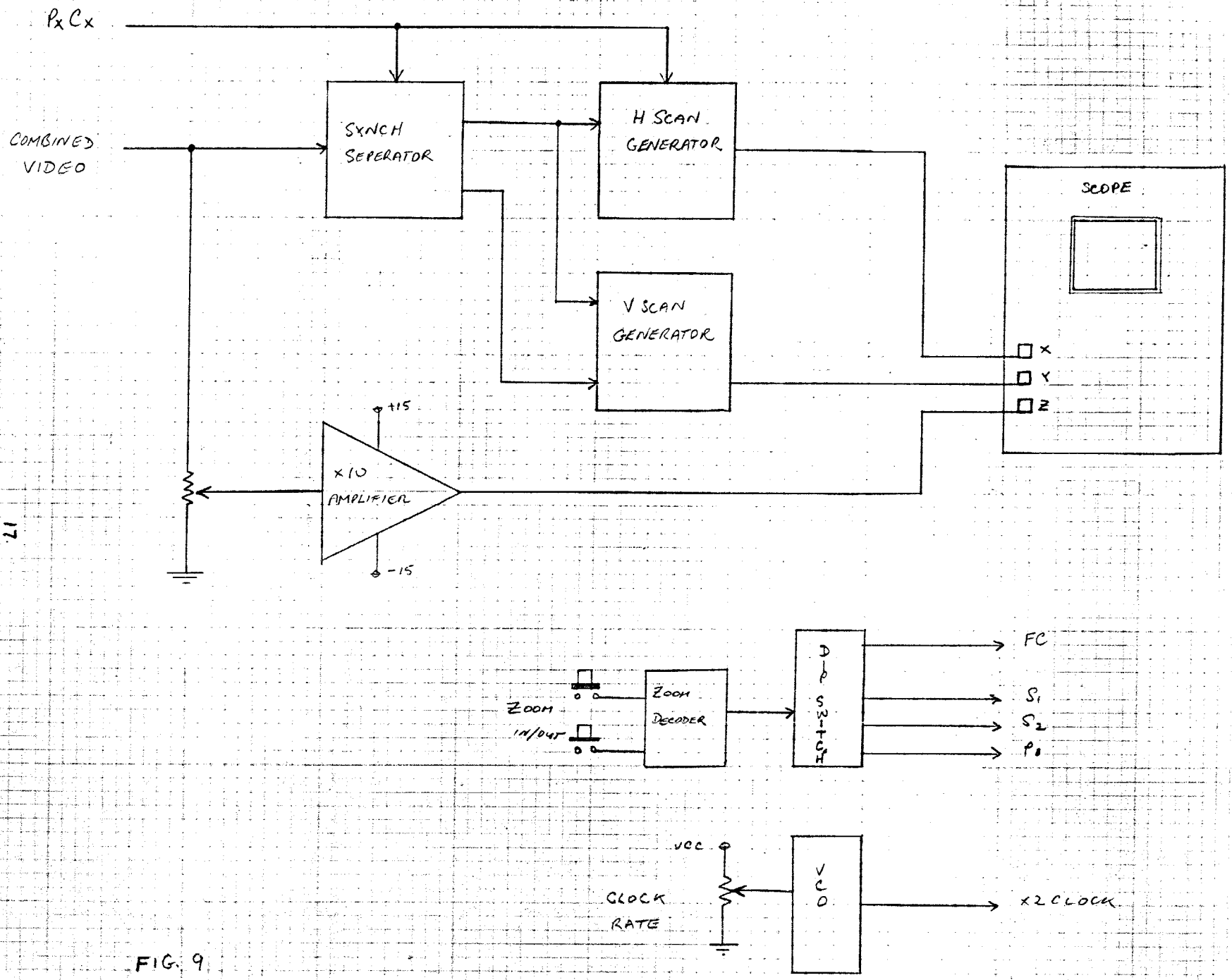

FIG. 9

S.V.D (SADOTA VIDEO DISPLAY)

BLOCK DIAGRAM

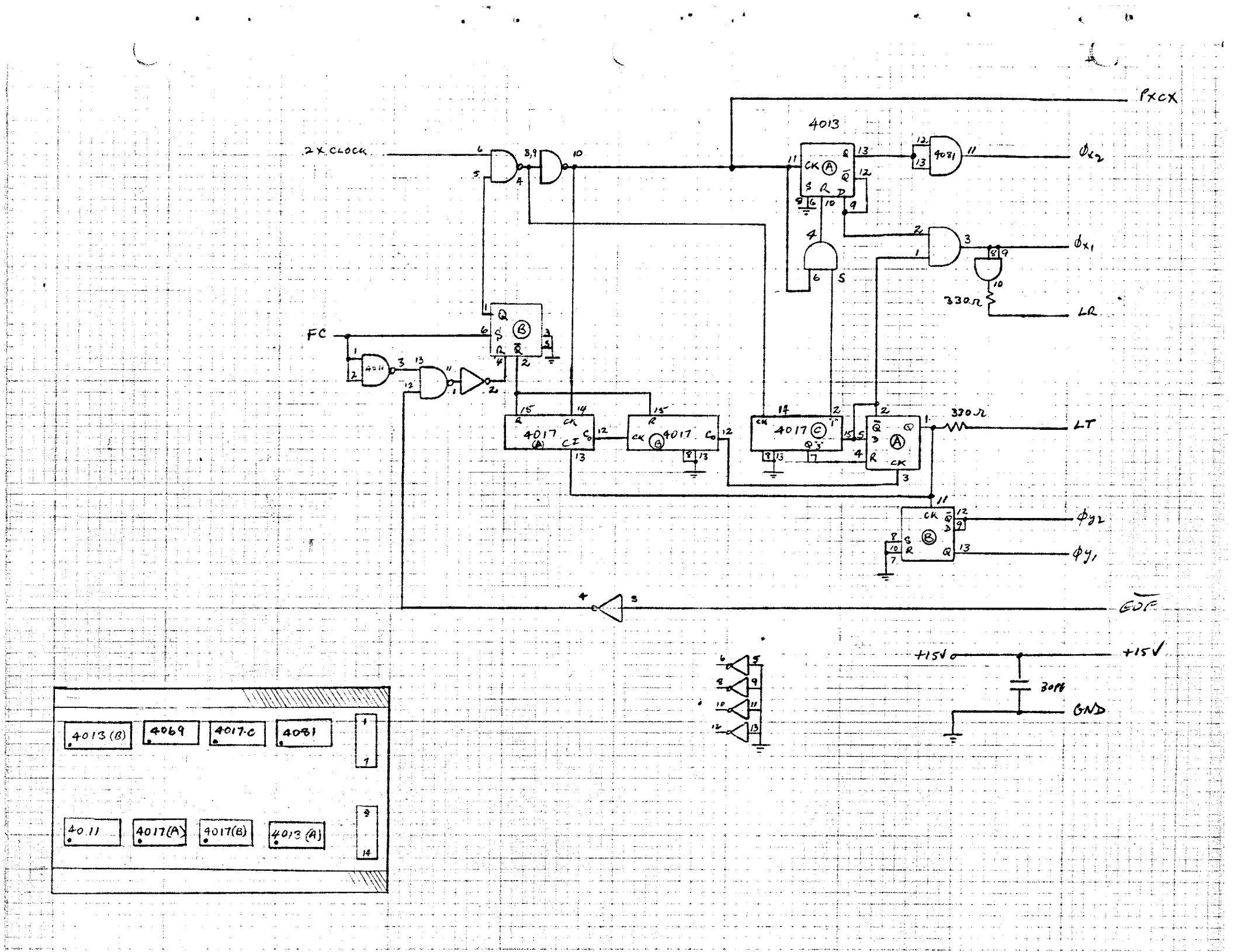
PXCX
4013
2X CLOCK
FC
4011
4017 (A)
4017 (B)
4017 (C)
4081
330Ω
LR
LT
ϕ_{x_2}
ϕ_{x_1}
ϕ_{y_2}
ϕ_{y_1}
EOF
+15V
+15V
30pF
GND
4013 (B)
4069
4017-C
4081
4011
4017(A)
4017(B)
4013 (A)

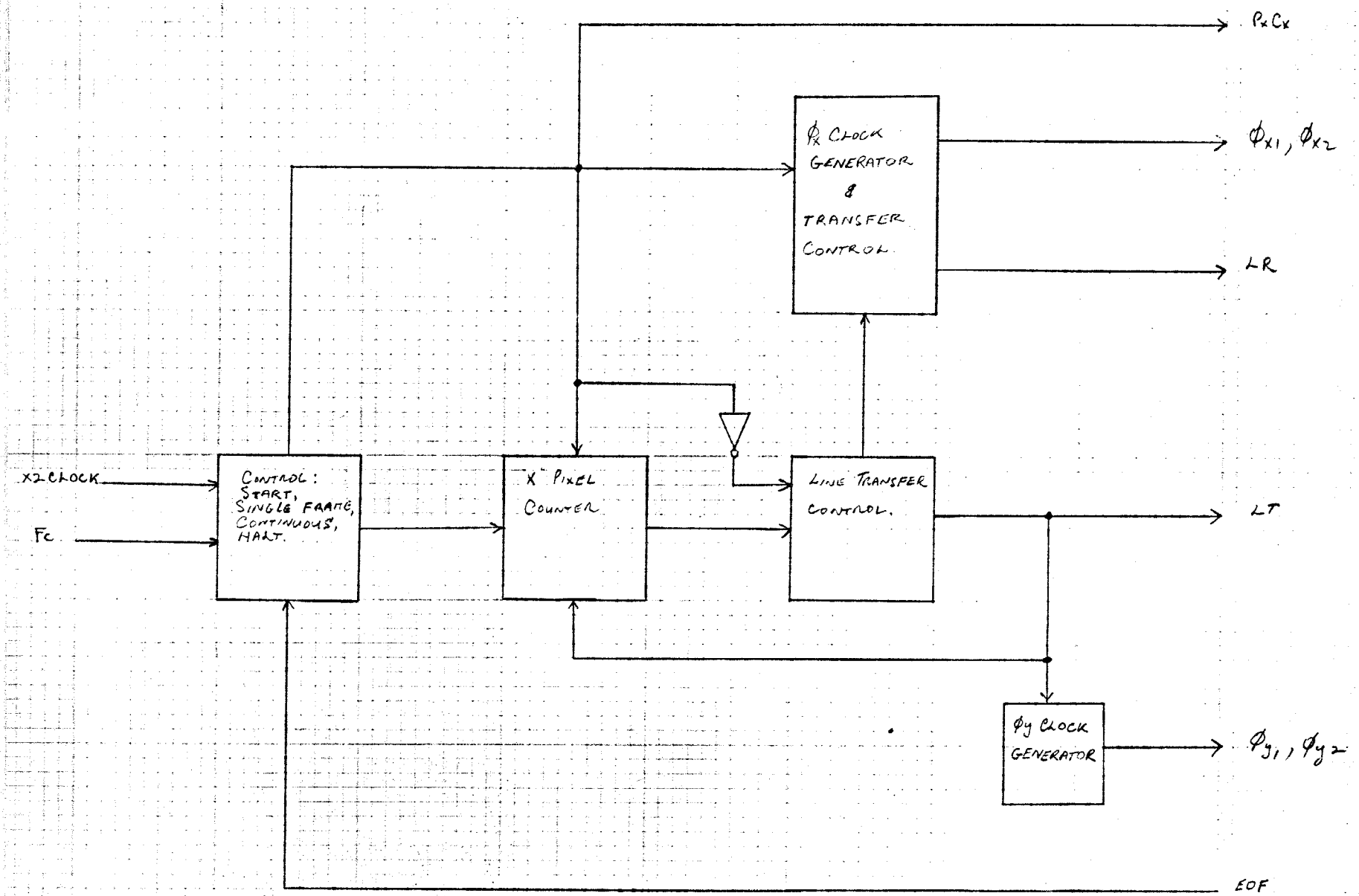

FIG. 11

TIMING BOARD (BLOCK DIAGRAM)

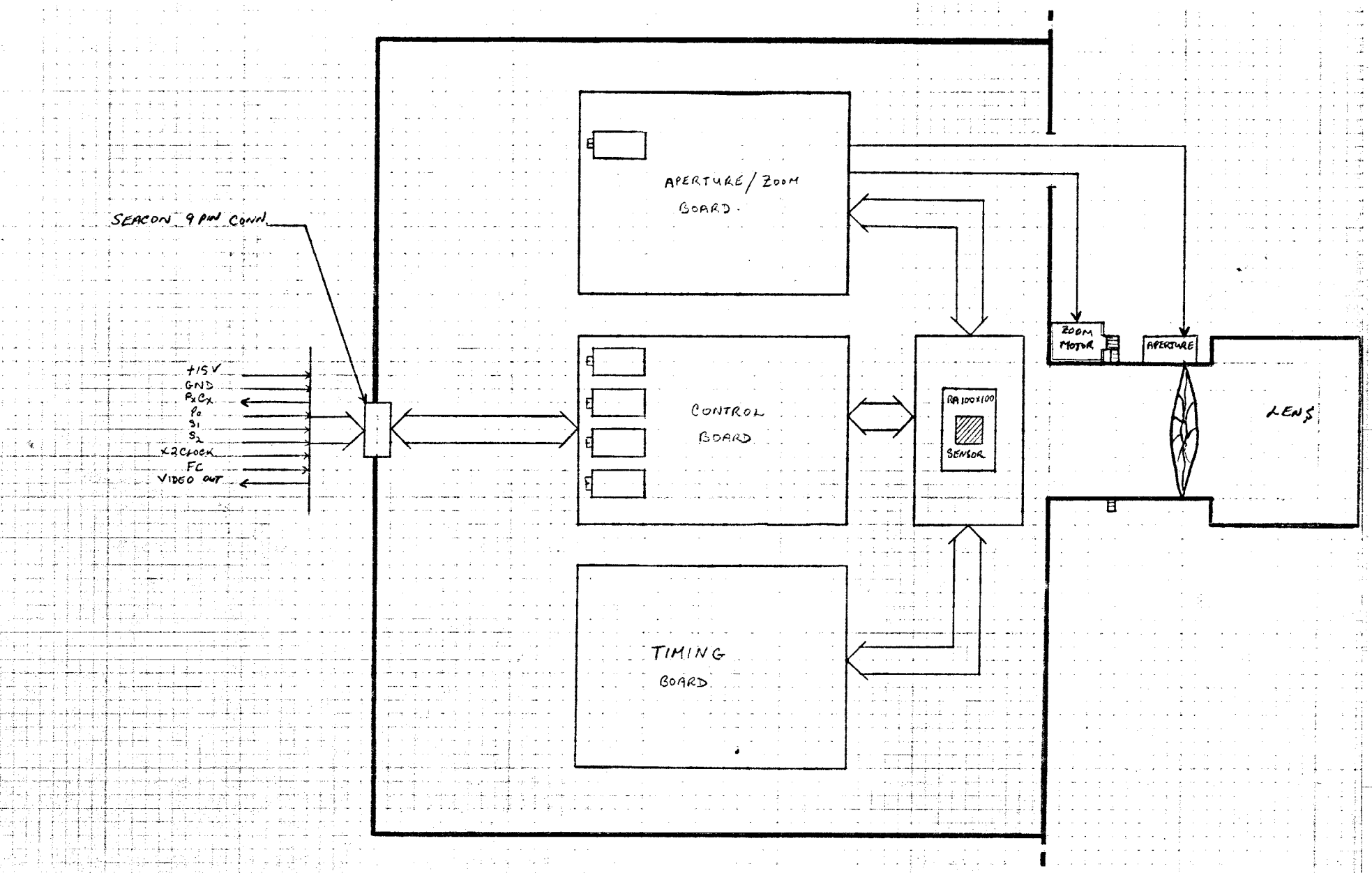

CAMERA BLOCK DIAGRAM

FIG. 12

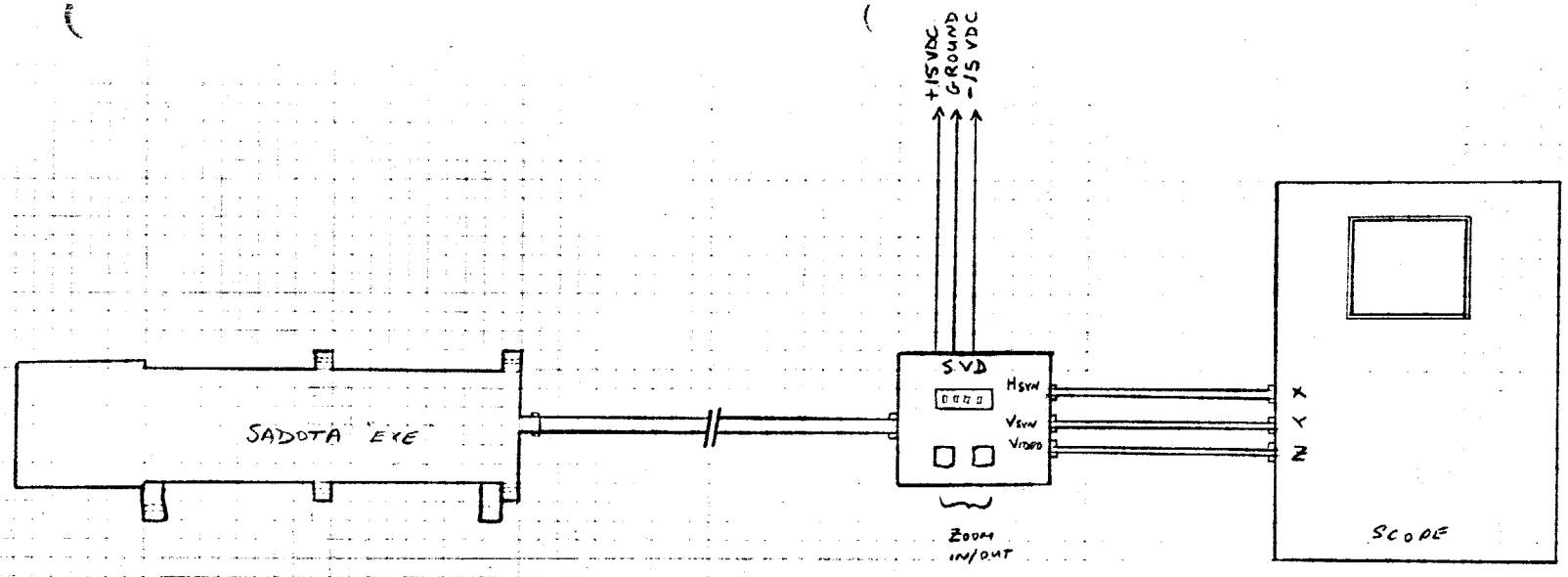

BASIC CONNECTION DIAGRAM

FIG. 13

CONTROL BOARD

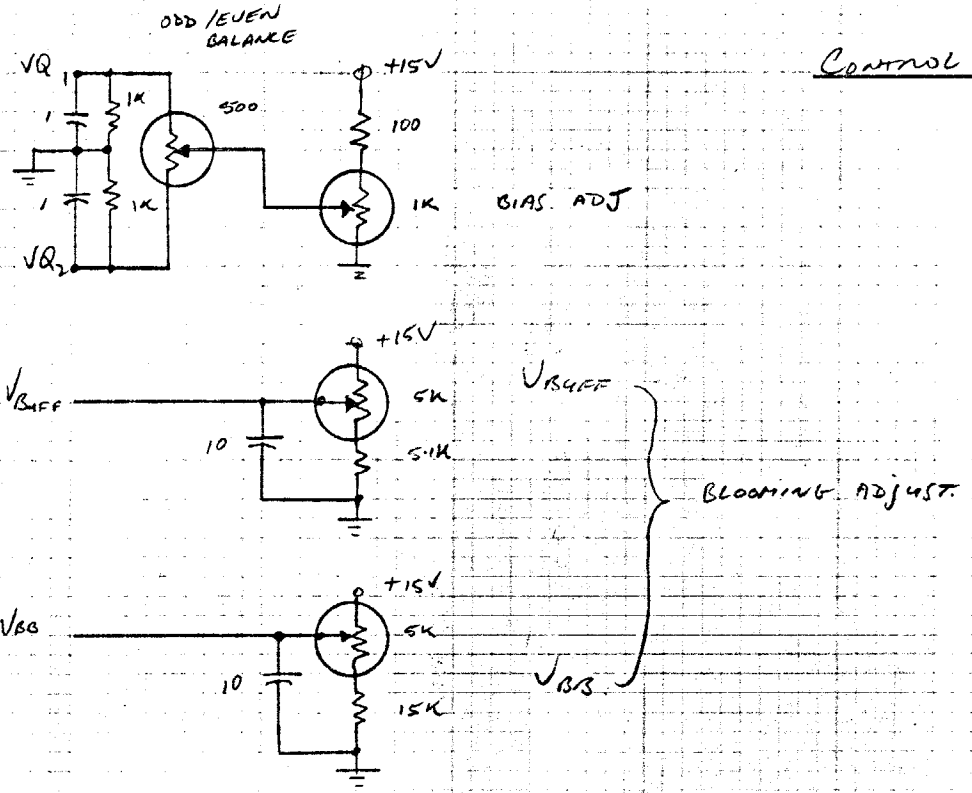

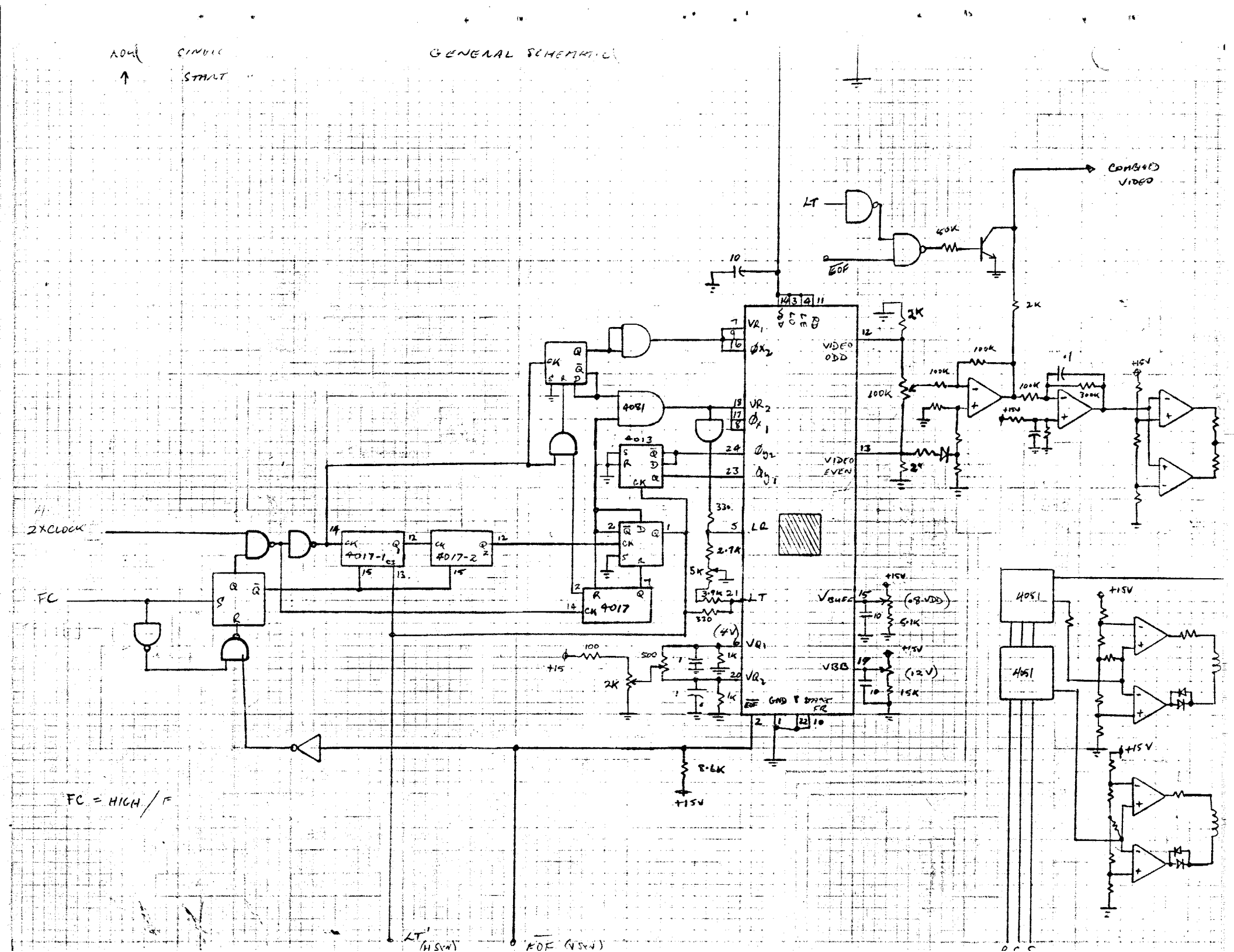
GENERAL SCHEMATIC
START
2XCLOCK
FC
FC = HIGH / F
4017-1
4017-2
4017
4013
4081
LT
EOF
COMBINED VIDEO
VIDEO ODD
VIDEO EVEN
+15V
8.6K
4051
4051
LT' (HSW)
EOF (VSW)

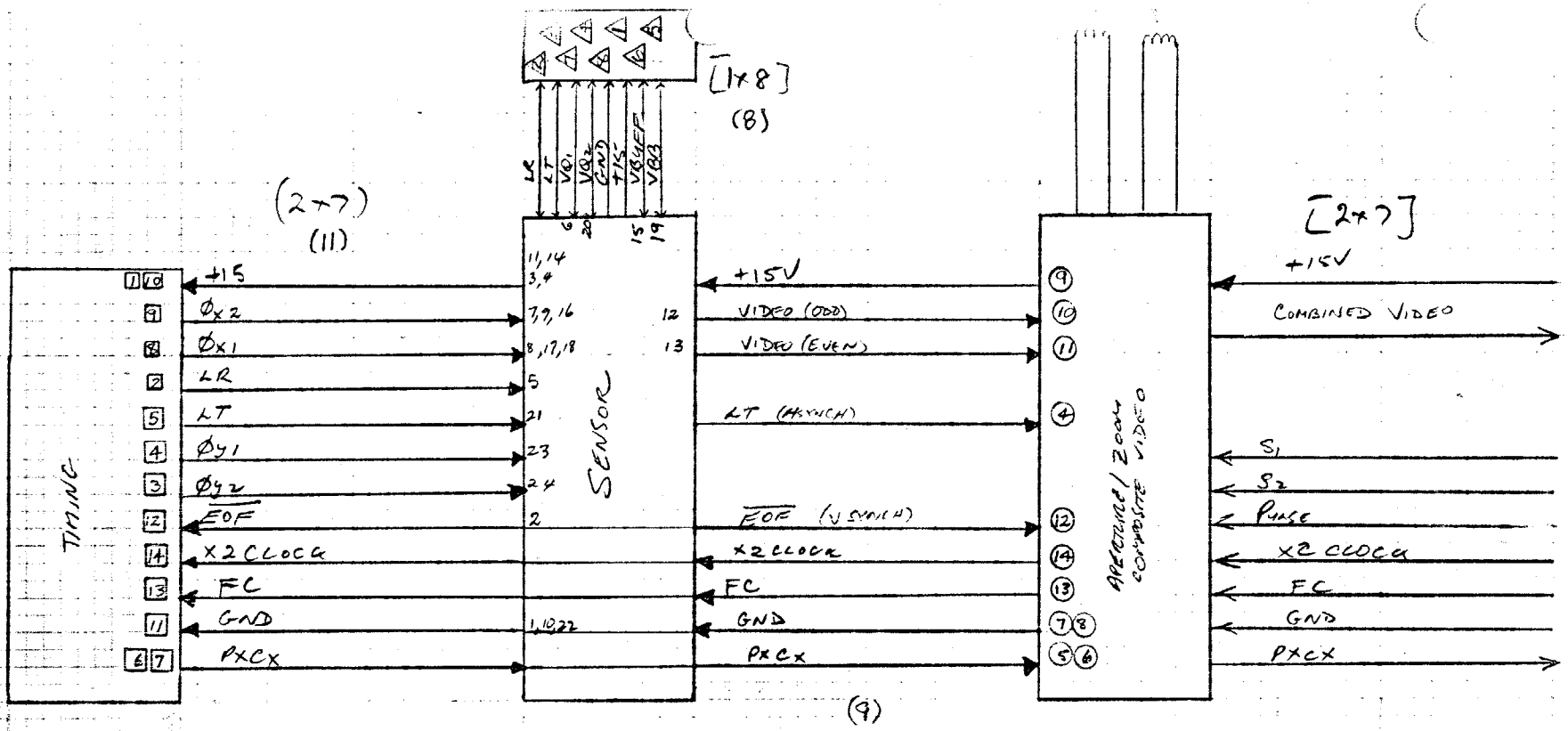

CAMERA BOARD INTERCONNECTION

AUTO APER. C / ZOOM
COMP. VIDEO.

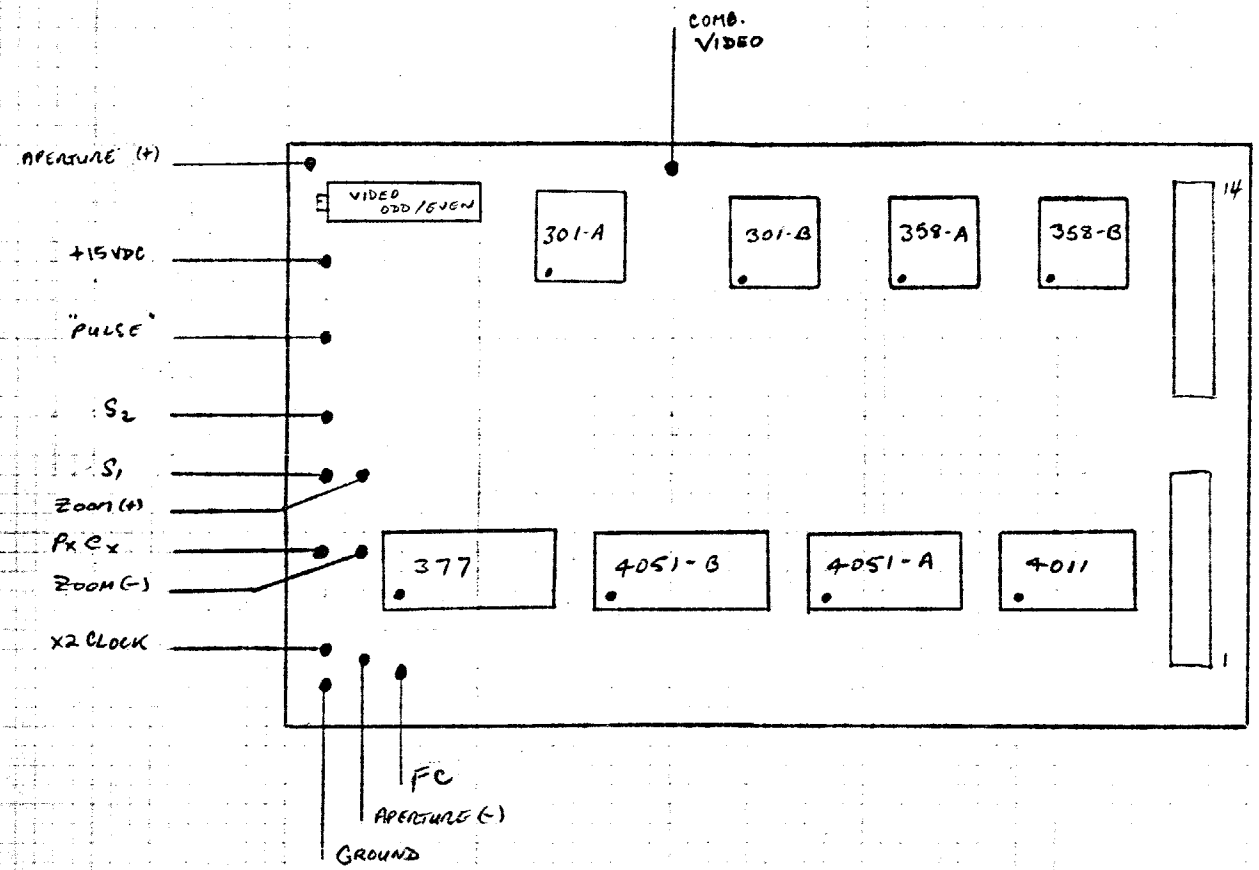

1. VIDEO (COMPOSITE)	1.	VIDEO INFORMATION (2VP'P) COMBINED WITH VERTICAL & HORIZ. SYNCH. PULSES.
2. FC	8.	FRAME CONTROL. POSITIVE EDGE STARTS FRAME, LOGIC 1 REPEATS; PULSE FOR SINGLE FRA
3. S_1	7.	(LSB) CONTROL INPUT FOR APERTURE / ZOOM CONTROL.
4. P_0	2.	(MSB) PULSE " " " "
5. GROUND	9.	
6. $R_x C_x$	6.	CAMERA CLOCK OUTPUT
7. S_2	3.	SEE S_1
8. 2X CLOCK	4.	CAMERA CLOCK INPUT
9. +15 VDC	5.	INPUT POWER TO CAMERA

AMP

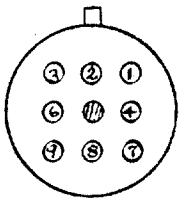

SEACON

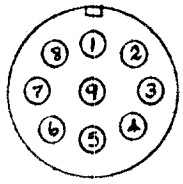

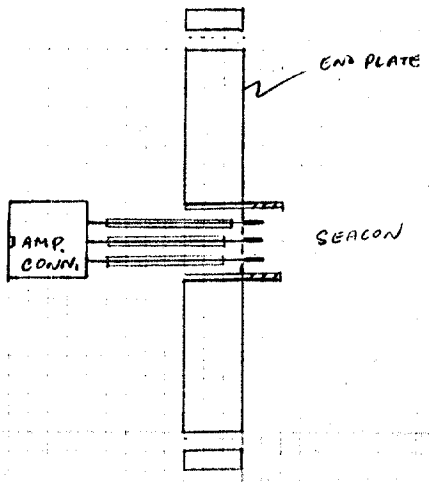

FIG. 17

APPENDIX A.

Preliminary Analysis Of The Components And Performance Of The Satoda Camera

H Sadjian.
General Sensors, Inc

I. Introduction

This preliminary analysis characterizes the expected optical performance and specific components of the underwater "eye" of project SATODA II.

The "eye" consists of a correcting viewing port, a camera lens and a CCD sensor with peripheral light source as, outlined in OEA proposal 479, dated May 18, 1979.

This preliminary analysis examines the performance of the "eye" in terms of:

1) field-of-view
2) sensitivity of the CCD
3) depth-of-field
4) resolution (approximate analysis)
5) intensity required

In addition, the components necessary are defined for:

1) viewing port
2) type of camera lens
3) correcting optics
4) type of light source

The more difficult analysis of the "eye" performance in different water types and a more exact analysis of the resolution in terms of object size, reflectivity etc., is relegated for the next report.

II. Viewing Port

Several undesirable effects are introduced by the use of a simple flat window. The most important are:

1) reduction of field-of-view
2) distortion and blurring of the image
3) change in effective focal length of camera lens

There are several methods used to correct some of the problems asso-

Originally, our intention was to have the dome made from acrylic plastic as it has been used at great depths successfully (see article on acrylic dome windows appendaged to this report). However, due to the cost of tooling for 1 or 2 windows, it was decided to use glass (BSC) as the material based on cost. It is expected that glass domes will perform similar to plastic domes with the added advantage of being easily cleaned.

Based on the expected field-of-view of the camera lens (next section), a dome with an inner radius of curvature of 3.5" is necessary. Based on the hydrostatic pressure anticipated using a safety factor of 10 (see appendaged report), a thickness of ½" is required. Hence we require a dome window with radius of curvature of 3.5", ½" thickness and a size that produces a 60° angle with the center of curvature.

In addition, a supplementary lens of about 1/4R or about +3 (2.8) diopters is to be attached to the camera lens. The combined camera lens and supplementary lens is to be positioned 3½" from the center of the dome window. See Figure 1.

III. Camera Lens and Field-Of-View

For a system to be used for exploration, it is desirable to maximize the field-of-view and resolution. In order to achieve this, a Zoom lens is necessary. As the sensor (next section) was originally designed for super-8 movie format (diagonal 7.2mm), we require a short focal length lens (for field-of-view) and a high zoom ratio for resolution (see section on resolution). Although high zoom ratios are avaible (e.g. Schneider lens, f/1.4, 12:1 zoom), a trade off between costs and performance has dictated the use of the power zoom lens manufactured by Bell & Howell (f/1.8 zoom).

The expected field-of-view as a function of lens focal length for this lens shown in figure 2. This is based on the diagonal demension of

7.2mm for the sensor.

IV. Sensor

Due to cost limitation, it was originally intended to use the Fairchild CCD-202. However, Fairchild no longer manufactures the sensor but has been replaced by a more expensive CCD-211. This device is larger and contains more photosites than the 202 (see data sheet appendaged to this report).

Although the appendaged data sheet was received a few weeks ago, we have learned from Fairchild that it is already outdated and Fairchild will becoming out with a new data sheet in the near future. They have apparently increased the responsivity and made some other changes.

The device comes in three different classes (A,B,C) depending on the number of blemishes. In addition, they manufacture a class below C which according to Fairchild means more blemishes than C but varies. At the time of order, they send the best available one.

V. Performance Calculations

A. Sensitivity of the CCD-211

In order to determine the intensity of light source to use for a given target, it is necessary first to determine the expected sensivity of the sensor. In these preliminary calculations, we take into account the water attenuation only (i.e. neglecting backscattering and water degradation of image).

The CCD-211 is an integrating device whose background (dark voltage) is a function of integration time and temperature. This dark voltage will limit the sensitivity and somewhat the dynamic range. In order to simplify the calculations, the CCD-211 can be treated as film in determining sensitivity. The dark voltage corresponds to film fog and integration time, exposure. In the ASA system used for films, a point .1 density above fog level (with a given gamma) is used as the reference point for determing speed. For the

CCD, this would correspond to voltage of 1.25 above dark voltage (since gamma is one). The speed is then determined from the expression,

$$S(ASA) = \frac{.8}{H} \qquad (1)$$

where H is the exposure in meter-candle-seconds (i.e. lumens/meter^2). The .8 factor is a safety factor of 20% from the minumum exposure point.

Before we can utilize (1), we need an expression for the dark voltage. According to Fairchild, the dark voltage increases linearly with integration time and exponentially with temperature (doubles every 7^{o}C). Based on the data sheet, for a clock frequency of 7.0 MH_z, the dark voltage is given as 0.6 mv. According to timing diagram, there are 250 pulses per horizontal line and 126 horizontal lines per each half of the picture. Hence there are 2(250)x(126) or 63,000 pulses per picture. Then the integration time (time per picture) is,

$$t_{int.} = \frac{6.3 \times 10^4}{f} \qquad (2)$$

Since dark voltage is linear with integration time then,

$$V_D = K\, t_{int.} = \frac{6.3 \times 10^4\, K}{f} \qquad (3)$$

The K is determined from the data sheet (V_D =.6mv at 7.0 M H) as 66.7. Hence,

$$V_D = \frac{4.2 \times 10^6}{f} \text{ (mv)} \qquad (4)$$

According to the data sheet, the f ranges from $.5 \times 10^6$ to 15×10^6 Hz. Hence the dark voltage should vary from V_D = 8.4 mv to .3 mv. Since the saturation voltage is typically 200 mv and the dynamic range is 300, the noise voltage should be about .67 mv. Hence the lower limit is set by the noise while the upper limit is set by the scan frequency. We can expect the V_D to vary from .6 mv at the high frequency end to 8.4 mv at the low frequency end. Finally, we multiply these values by 1.25 (corresponding to a density of .1 above fog for film) to obtain .75 to 10.5 mv.

Hence we can write that,

$$V_D = \frac{1.25(4.2\times10^6)}{f} = \frac{5.25\times10^6}{f}\,(mv) \qquad (5)$$

for $f < 7MHz$.

In order to use (5) to determine the equivalent ASA speed, we need the responsivity of the CCD. The data sheet gives the responsivity as 1.0 $V/\mu J/cm^2$ of tungsten light at 2854°K filtered through a Corning 1-75 IR filter. However, Fairchild has told me that the new spec sheets will indicate a responsivity of 5.0 $V/\mu J/cm^2$.

We anticipate that the light source that will be used will be a high intensity flash unit which operates at about 6000°K. Consequently, we require the calibration in terms of this light source.

Unfortunately due to the way the CCD is calibrated, it was necessary to numerically integrate the light source distribution against the detector sensitivity with the 1-75 filter. This was done as follows: the responsivity is given by,

$$R\left(\frac{V}{\mu J/cm^2}\right) = S_P\left(\frac{V}{\mu J/cm^2}\right)\frac{\int W\times F\times D\,d\lambda}{\int W\times F\,d\lambda} \qquad (6)$$

where Sp is the peak responsivity of the CCD and W represents the tungsten light disribution, F the filter transmission and D the relative detector sensivity. The integration was performed from 380 to 1200 nm (the limits of the detector sensitivity).

The value of the integral ratio is 0.40. Hence Sp is 12.5 $V/\mu J/cm^2$. Using (6) we can find the response of the CCD to 6000°K blackbody light (BB) from

$$R_{BB}\left(\frac{V}{\mu J/cm^2}\right) = 12.5\int BB\times F\times D\,d\lambda \Big/ \int BB\times F\,d\lambda \qquad (7)$$

The value of the integral ratio was found to be .26 which makes R_{BB} = 3.25 $V/\mu J/cm^2$.

To use these values for computing the equivalent ASA, we convert the

objective units (μJ) to subjective units (lumen-secs) used in characterizing both flash units and film speed.

For tungsten light there are about 19 lumen-secs per joule. Hence there are about .018 foot-candles per $\mu J/cm^2$ of total tungsten light. Numerical integration of filtered to total tungsten light gave a value of .097 or 10.2 $\mu J/cm^2$ total per 1 $\mu J/cm^2$ filtered. This gives about .18 foot-candle-secs (fcs) per $\mu J/cm^2$ filtered light. Using this conversion and the given responsivity means that the equivalent subjective responsivity is 27.2 volts/fcs.

Similarly for blackbody light of 6000°K, there are about 92 lumen-secs/watt or .085 fcs/$\mu J/cm^2$ of total BB light. The ratio of filtered to total light was found by numerical integration to be 0.355. Hence there are 2.81 $\mu J/cm^2$ total light to 1 $\mu J/cm^2$ filtered light. Combining this the luminous efficiency for BB we have about .24 fcs per $\mu J/cm^2$ filtered light or a responsivity of 13.6 V/fcs.

In order to use this value for computing the ASA speed, we convert this to meter-candle-seconds (mcs) and use the reciprocal of the responsivity to obtain that luminous response of the CCD-211 is 0.8 mcs/volt. Combining this with (5) we have that, the limiting sensitivity is given by,

$$H(mcs) = 4.2 \times 10^6 / f(Hz) \qquad (8)$$

Combining this with (1), we have that,

$$S(ASA) \cong 1.5 \times 10^{-4} f(Hz) \quad f < 7\,MHz \qquad (9)$$

This expression is for blackbody light of 6000°K. Since the f varies from $.5 \times 10^6$ to 7.0×10^6, the speed will vary from 75 ASA to 1050 ASA.

These values will be used on the next section to calculate the guide number necessary to obtain satisfactory exposures. It is to be cautioned that expression (9) is approximate as it was derived from the values from the data sheet on the CCD-211 which are approximate.

B. Calculation of Guide Number For Flash Unit

In photography the guide number (GN) is used to characterize flash unit for given film speed. It is a useful number as th GN divided by the distanc to the subject yields the f/number necessary to obtain an exposure. For unde water illumination, we utilize this parameter except we take into account the attenuation due to water.

For a source characterized in terms of beam candlepower·sec (BCPS), a subject a distance R from the source will receive an illumination level of I/R^2 attenuated by the water path by $e^{-\alpha R}$ where α is the water attenuation coefficient. If we assume a diffuse reflectivity ρ for the subject, the effective brightness (B) of the subject will be,

$$B = \frac{I(BCPS)}{\pi R^2} \cdot e^{-\alpha R} \rho \tag{10}$$

The illumination level produced in the image plane by a camera lens characterized by its' f/number, lens transmission, and the attenuation of the water path is,

$$H = \frac{\pi B}{4 f\#^2} \cdot e^{-\alpha R} \cdot T \tag{11}$$

Combining (10) and (11) we have that,

$$H(\text{image plane}) = \frac{I(BCPS) e^{-2\alpha R} \rho T}{4 (f\# R)^2} \cdot \left(\frac{N_i}{N_o}\right)^2 \tag{12}$$

The factor $(N_i/N_o)^2$ represents the illumination level change due to the fact that the subject is in water and the image is in air.

From equation (1) where the speed of the sensor was .8/H, we have that,

$$S = 3.2 (f\# R)^2 N_o^2 / e^{-2\alpha R} I \cdot \rho T \cdot N_i^2 \tag{13}$$

The (f#R) factor is the GN. Solving for GN, we have,

$$(GN)_W = \frac{N_i}{N_o} \sqrt{\frac{S \cdot I \cdot \rho T e^{-2\alpha R}}{3.2}} \tag{14}$$

For photography in air, $N_i = N_o$, $\rho = .18$ and $T = .9$ and $\alpha = 0$, hence,

$$(GN)_{AIR} = \sqrt{\frac{S \cdot I (.18)(.9)}{3.2}} \tag{15}$$

Since the GN values of light sources are expressed in feet, the necessary f# becomes about 92/32.8ft. or an f/2.8. This is an acceptable f# but will suffer from a restricted depth-of-field as will be shown in the next section

In summary, the f# to be used becomes a strong function of the water clarity and has to be determined from the expected scenario. Again we note that these equations are approximate as the sensor data are approximate. In addition, these equations are based on an average reflectivity of 18%. For low reflectivity objects (< 10%) the equations are correspondingly modified.

C. Depth-Of-Field Calculations

In the previous section we derived the expressions relating the necessary f# to the scan frequency of the sensor, the range, the light source and the attenuation coefficient. For underwater surveillance, the focus and f# cannot easily be changed. It then becomes desirable to maximize the depth-of-field so that refocussing or motion of the vehicle is not excessive.

The expressions relating the depth-of-field (DOF) are given by,

$$d_{MAX}/d = 1 \Big/ 1 - a\left(\frac{f\#}{F^2}\right)(d-F) \qquad (19)$$

and

$$d_{MIN}/d = 1 \Big/ 1 + a\left(\frac{f\#}{F^2}\right)(d-F) \qquad (20)$$

where d_{max} = maximum distance object is in acceptable focus

d_{min} = minimum distance object is in acceptable focus

a = diameter of circle of least confusion (i.e. minimum acceptable blur circle)

f# = f number

F = focal length of camera lens

d = distance for which camera is focused

From equation (19) we let d/F =D and ϕ = f#/F(mm) and rewrite as,

$$d_{MAX} = DF / 1 - a\phi(D-1) \qquad (21)$$

Solving for D,

$$D = (1 + a\phi) / \left(\frac{F}{d_{MAX}} + a\phi\right). \qquad (22)$$

Equation (20) becomes,

$$d_{MIN} = DF / 1 + a\phi(D-1) \qquad (23)$$

In air photography, the hyperfocal is that distance for which the camera must be focused so that the camera is in focus from infinity to the some point near the camera lens. For situations where the camera cannot be re-focused, the hyperfocal setting is used. For $d_{max} = \infty$, equation (22) becomes,

$$D_\infty = 1 + \frac{1}{a\phi} \qquad (24)$$

and d_{min} is just d/2. In water photography, the maximum distance is not infinity but a distance dicated by the water clarity, sensor sensitivity and light source intensity. Consequently, we need to slove the d expressions for different d_{max} distances.

According to the data sheet, the limiting horizontal resolution is about 190 TV lines. As there are two TV lines per optical line pair and the image format is 5.7mm, the limiting spatial frequency is about 14 line pairs/mm. We take as the diameter of the acceptable blur circle the reciprocal of this or about .07mm (see next section). Letting β represent F/d_{max} (β varies from 0 to 1), we rewrite equation (22) as,

$$D = (1 + .07\phi) / (\beta + .07\phi) \qquad (25)$$

This equation is plotted in figure 5. The Bell & Howell lens focal length varies from about 8mm to 64mm and the f# from 1.8 to about f/22. Hence the ϕ in equation (25) varies from about .02 to about 3. As ϕ goes to zero (i.e. low f# and long focal length) the D approaches $1/\beta$. Once the D is obtained which defines d, the distance for which the lens is focussed, the

d_{min} is obtained from,

$$d_{MIN} = \frac{DF}{1 + .07\phi(D-1)} \qquad (26)$$

We have not plotted this equation as it involves three variables and can be computed easily once the D, ϕ and F are defined.

As an example of the use of the curve in figure 5, we continue the example given in the previous example. There we found that at 10 meters (32.8 feet), the f# required was f/2.8. Assuming a wide-angle focal length (8mm) we have that ϕ = .35. If the maximum distance is 10 meters, β = 8/10,000 or approximately zero. Hence $D = \frac{1 + .0245}{.0245} \cong 42$. Then d is .33 meters and $d_{MIN} \cong$ .33 meters/2 or .17 meters. Consequently, with the camera focussed at .33 meters, it will be in sufficient focus from 10 meters to 0.17 meters to match the sensor horizontal resolution.

In summary the DOF is a function of focal length, f#, sensor resolution and the maximum distance that the object is to be in focus. This effective hyperfocal distance maximizes the DOF.

D. Estimation of Sensor Resolution

The variables that go into the resultant resolution are both optical and electronic. For this preliminary analysis we only estimate the resolution and leave for the next report the complex problem of sensor resolution.

For the CCD-211, the vertical and horizontal resolution are different due to the structural make-up of the sensor (see data sheet). Consequently, for underwater use where orientation of the object cannot be controlled, we use the limiting horizontal resolution as the limiting resolution of the sensor (i.e. horizontal is less than the vertical).

From sampling theorem, if an image (or object) is sampled at fixed intervals (as is the case for the horizontal sensing elements of tht CCD-211), then the highest spatial frequency that can be passed without distortion is given by,

$$\nu_{MAX} = \frac{1}{2X} \qquad (27)$$

where x is the seperation of the sampling. For the CCD-211, the sensor sites are 30μ apart; consequently, the ν_{max} should be about 16.7 line pairs/mm. Based on the structure of the CCD, there are 190 TV lines per 5.7mm or 80 lines pairs per /5.7mm which is about 14 line pairs per mm. The data sheet shows two different horizontal resolutions depending on load resistance and shows a limiting value of 142 lines/picture height or 12.5 line pairs/mm. This degradation may be due to efficiency of transfer and scanning rate and the manufactures is not certain of the relationship.

However, for this analysis we use the 14 line pairs/mm as the limiting resolution and reserve the improvement in the accuracy for a future report. As a result, we may be underestimating the sensor resolution.

For this report, we postpone the degradation of the image due to water clarity. The relationship between sensor resolution and object resolution will be given by,

$$\nu_o = \nu_s \, F/R \qquad (28)$$

where ν_s is the limiting sensor resolution, F the focal length or image plane distance and R the object range. Hence, the resolution that can be recorded on the sensor is a function of both the focal length of the lens chosen and range to the object. This would seem to indicate that to maximize resolution, and to maximize the field-of-view, we need a zoom lens with the maximum zoom ratio consistent with cost.

For the zoom lens recommended for this work ($\sim$ 8mm $\longrightarrow$ 64mm), the resultant expected object resolution is shown in figure 6.

2. Sears & Roebuck Co.

Bell & Howell makes the movie cameras for Sears and is using this lens. It is the Sears model #9198. Perhaps you can get it more eaisily by buying the entire camera locally. App. cost is $250.

3. K-Mart

K-Mart has been advertising a Bell & Howell movie camera with an 8:1 zoom. I haven't seen it but I believe it is the same camera lens. It is selling here for about $150.

D. Sensor

There is no choice on the CCD-211 sensor. Fairchild is no longer manufacturing the CCD-202. There are 4 classes,A,B,C and a class designated as SL62935 which is less than C. The extent of the blemishes vary and when you order it, they send the best available one.

E. Flash Unit

The flash unit guide number (GN) should be as high as possible consistent with cost limitations and power limitations. As indicated in the section on guide number, the necessary (GN) is a strong function of operating range and water clarity.

You can use the Toshiba underwater flash unit with an air (GN) of 82(ASA 100) but is designed for 400 feet. With an α of .2 (typical of clear coastal waters) and a range of 3 meters and running the CCD at its lowest frequency, the resulting (GN) is about 30 in water. This means that you need an f# of about 2 which is at lower limit of the camera lens.

If possible, I would suggest that one of the Sunpak or Vivatar flash units be used with the (GN) a 100 or more. Then you can use the housings that are make for these units by Ikelite. Any of these flash units can be obtained from most camera stores.

If you can define the scenario to be used in testing this system, I'll be better able to define the flash unit necessary.

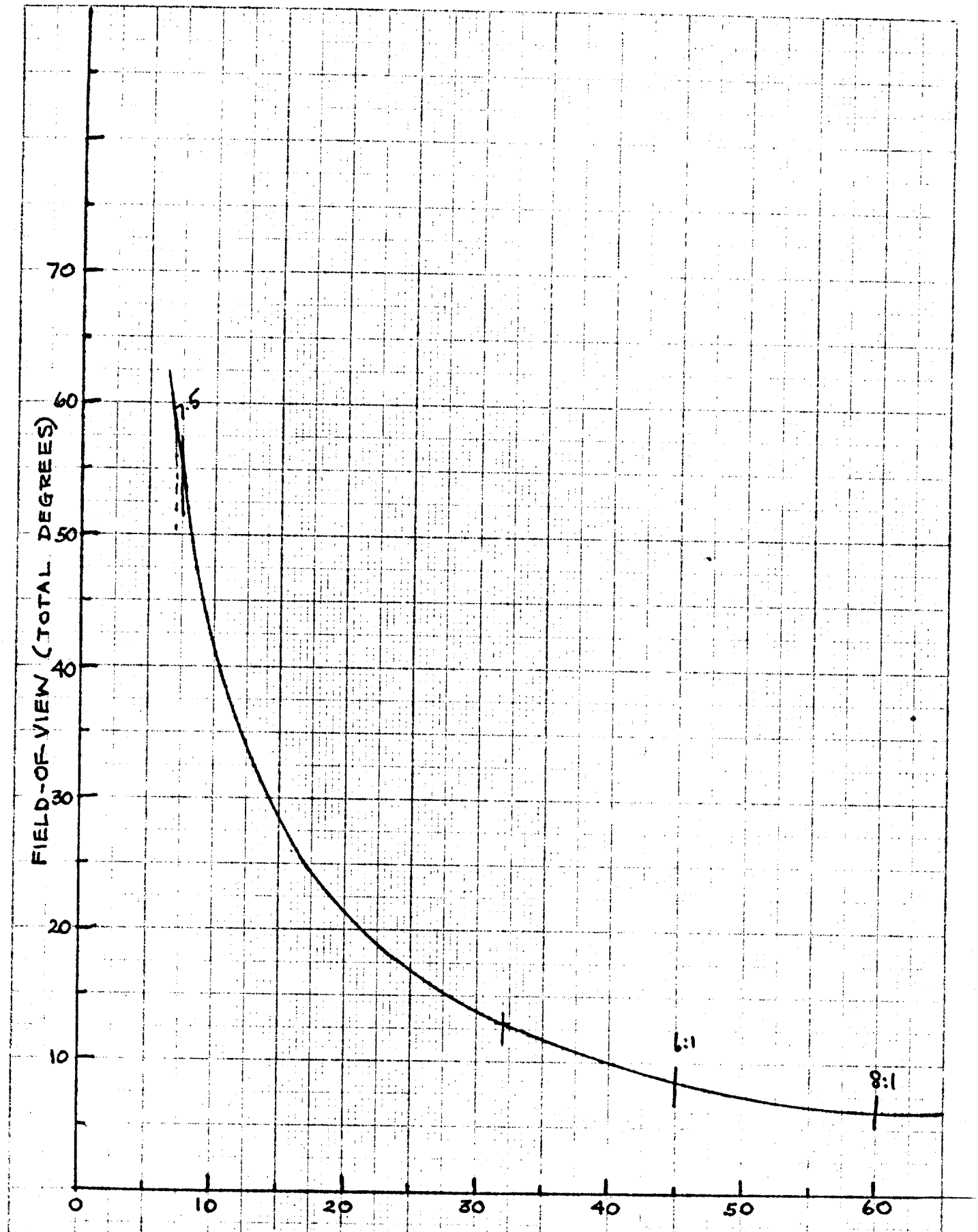

FIGURE 2. FIELD-OF-VIEW AS A FUNCTION OF LENS FOCAL LENGTH

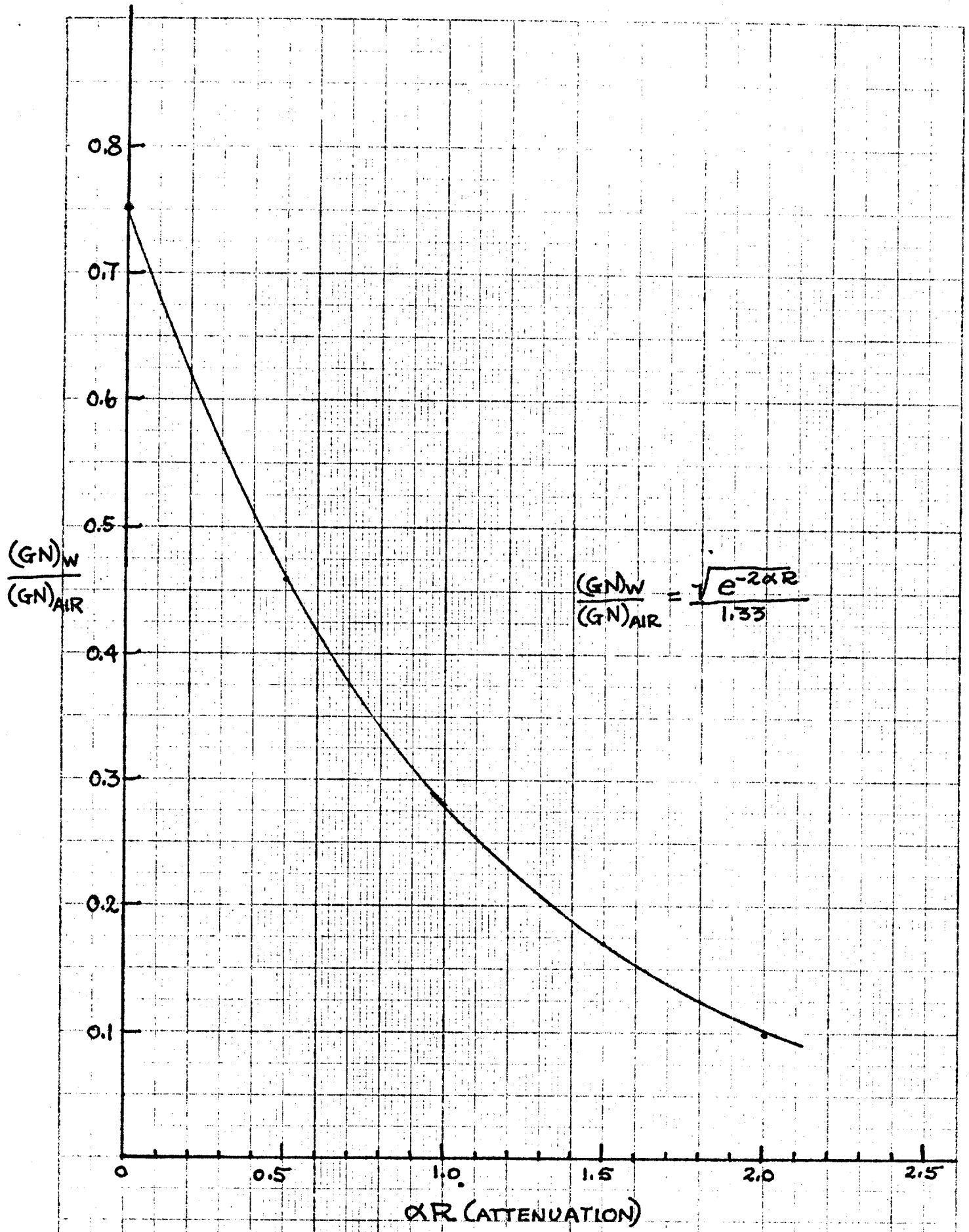

FIGURE 3. EFFECT OF WATER ATTENUATION ON GUIDE NUMBER (GN)

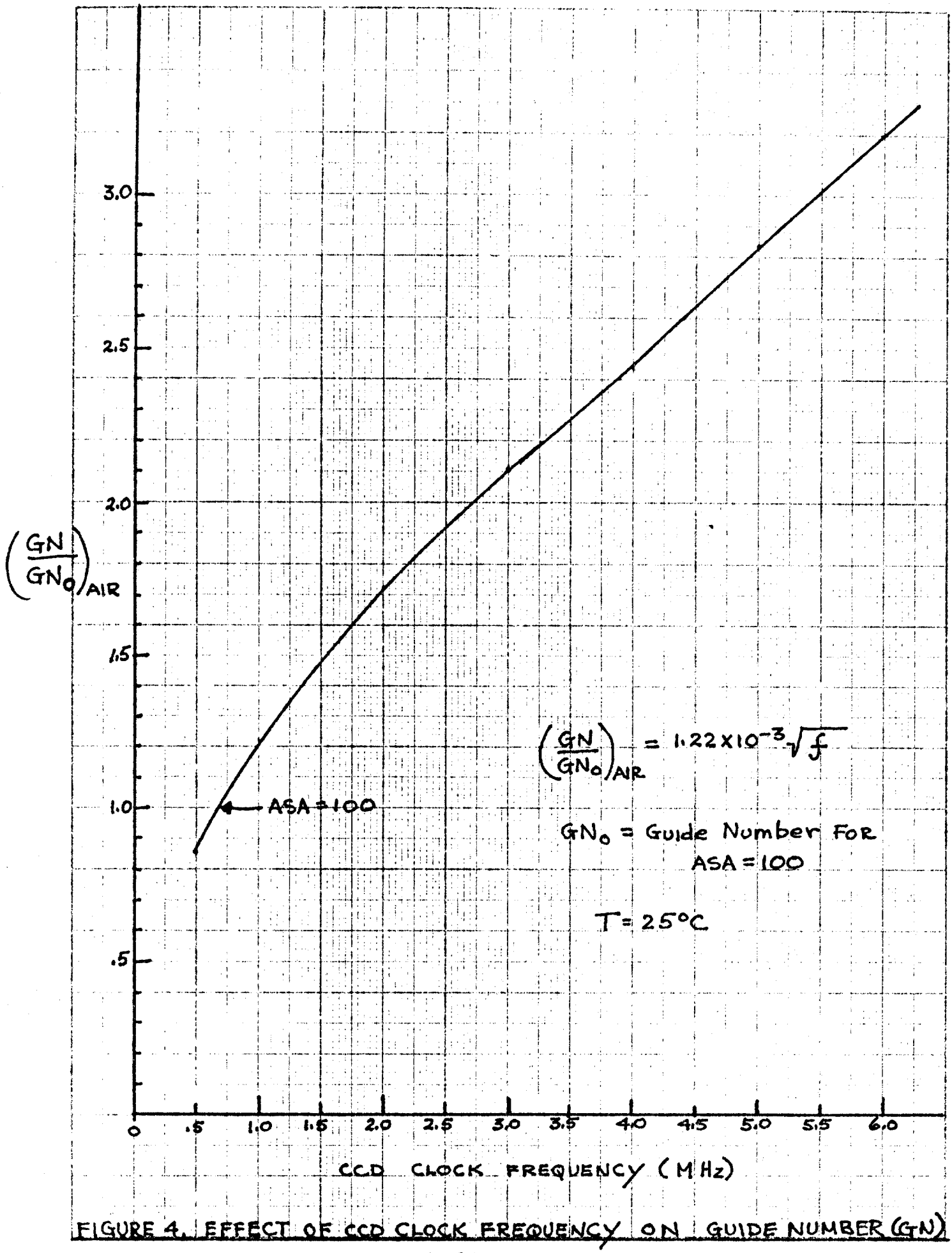

FIGURE 4. EFFECT OF CCD CLOCK FREQUENCY ON GUIDE NUMBER (GN)

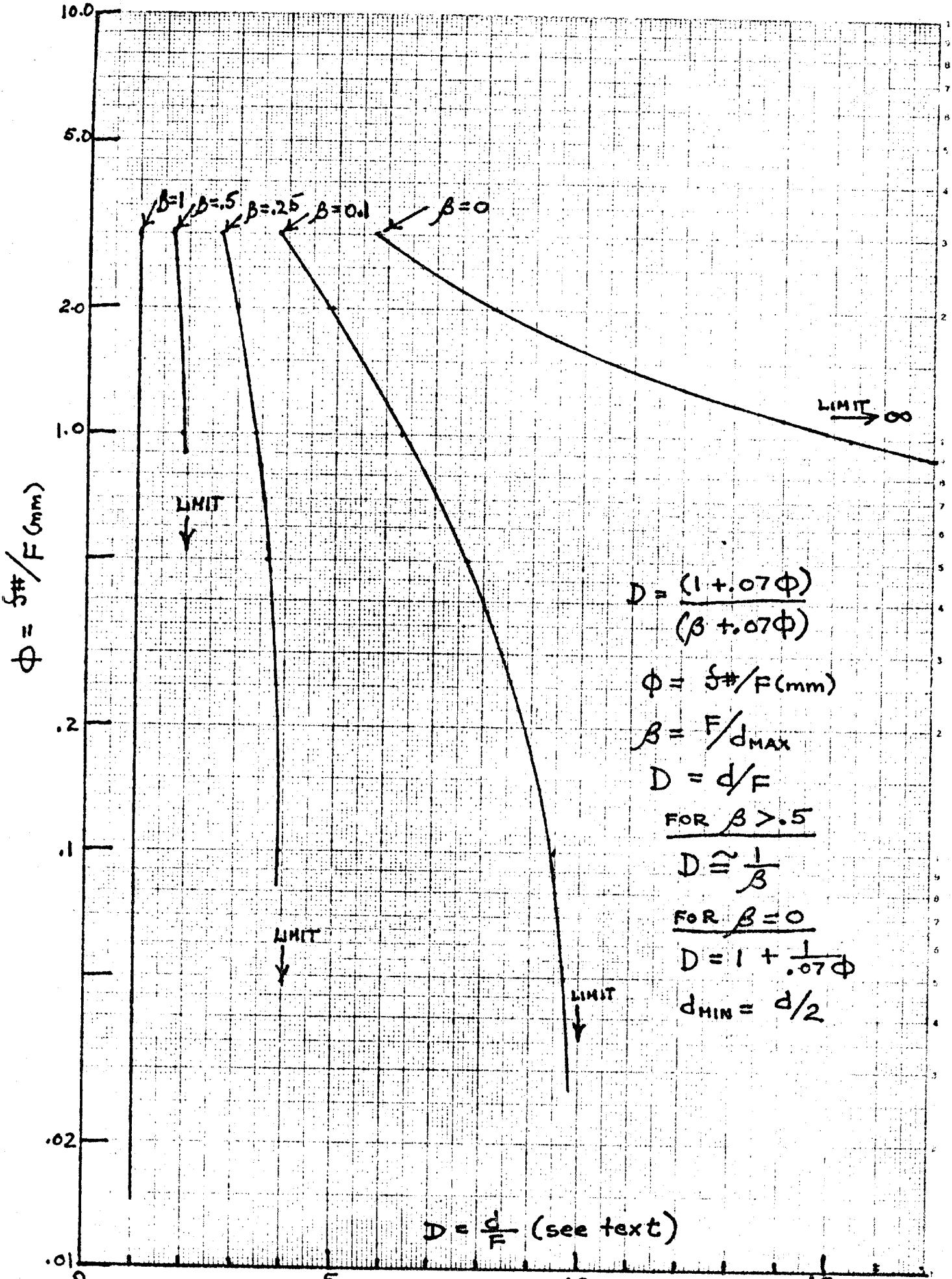

FIGURE 5. EFFECT OF F# AND F ON UPPER LIMIT OF DEPTH-OF-FIELD

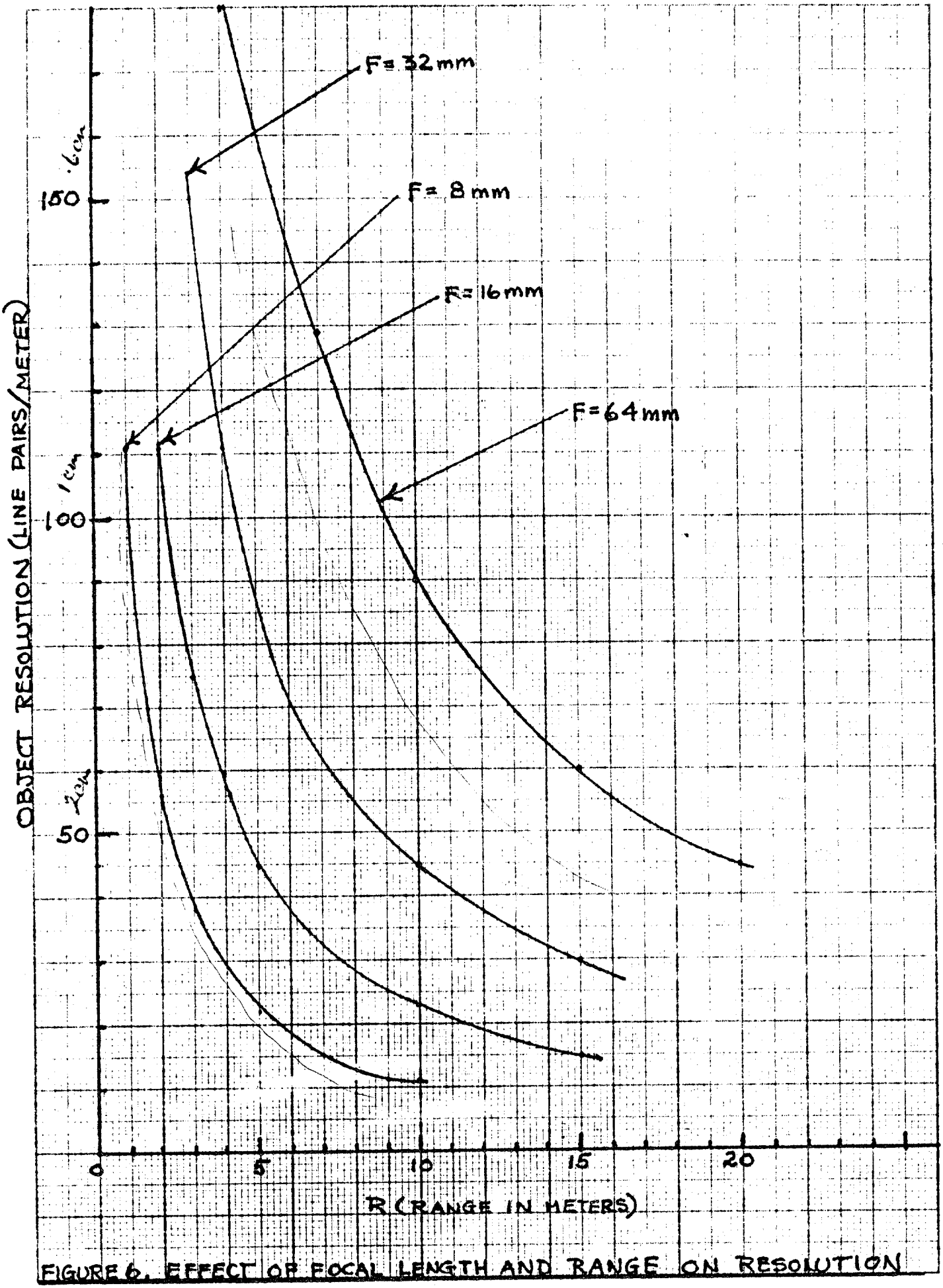

FIGURE 6. EFFECT OF FOCAL LENGTH AND RANGE ON RESOLUTION

APPENDIX B.

Analysis Of The Effect Of Water Clarity On The Performance Of The Satoda Camera

H Sadjian.
General Sensors, Inc

I. Introduction

This second analysis, in support of project SATODA II, examines three water types (defined below) in terms of the expected reduction of contrast. The reduction in contrast from a reflective target is the result of three factors:

(1) forward scattering (image degradation)

(2) attenuation

(3) backscattering

The water backscattering reduces the original target contrast while the attenuation and forward scattering degrade the image also in terms of contrast.

The results of this analysis are only to be used as a guide as water characteristics vary over a wide range and the results are approximate. The effort needed for exact solutions for different scenarios are not warranted and are only of academic interest.

II. Variables That Characterize Water Clarity

In order to predict the effect of water type on image quality, it has been found that the optical properties of water that best describe image degradation are:

(1) attenuation coefficient (α)

(2) small angle scattering coefficient (S)

(3) slope of the scattering curve for small angles (N)

(4) backscattering function (σ_B)

The first three parameters determine image degradation due to forward scattering and attenuation, while property (4) degrades the image due to contrast loss.

A. Image Degradation Due To Forward Scattering And Attenuation

Image degradation can be more easily calculated if the modulation transfer (MTF) function of sea-water is used rather than the spread function. A detailed analysis of the derivation of the MTF for sea-water is described in reference (1). There it is shown that the MTF can be written as,

$$\tau(\omega, R) = e^{-\alpha R} e^{S R \Sigma(\omega)} \qquad (1)$$

where ω is the spatial angular frequency expressed in radians (spatial frequency)/radians (angle). The α and S are defined above and the $\Sigma(\omega)$ is a series expression depending on N, the slope of the small angle scattering curve. For the type of waters encountered, N varies from 1.0 to 1.7. Due to the difficulty in solving the series solution, we have chosen a value of 1.00 for N for all the water types in this approximate analysis as the additional accuracy obtained by exact solutions is not warranted by the other approximations made in the report. For N=1.00, it has been shown (1) that the MTF expression has the closed form,

$$\tau(\omega, R) = e^{-\alpha R} e^{S R H(x_o)} \qquad (2)$$

where $H(X_o) = \int_o^{x_o} J_o(x)\, dx \,/\, x_o$

R=Range

Here the X_o equals $\epsilon\omega$ with ϵ the small angle limit considered in the scattering. In this report, the small angle limit is taken as .02 radians ($\sim 1.1^o$) as for most waters, a single slope defines the volume scattering function as least up to 1.1^o. The small angle

scattering coefficient then is defind from,

$$S = 2\pi \int_0^{\epsilon} \sigma(\theta)\, \theta\, d\theta \qquad (3)$$

where $\sigma(\theta)$ is the scattering function. The function $H(X_o)$ can be approximated for values of $X_o < 1$ (~ 1.00) and for values of $X_o > 10 (\sim 1/X_o)$. Consequently with given values of α, S, and N, the MTF can be obtained as a function of R.

For the special case of the CCD sensor to be used in this project, the limiting resolution by the sensor is about 14 cycles/MM at 50% contrast. In terms of the focal length of the camera lens the angular spatial frequency ν (cycles/radian) will be given by,

$$\nu = 14F(mm) \qquad (4)$$

where F is the focal length of the camera lens. Assuming we have a zoom lens varying from about 8mm to 50mm in focal length, the ν will vary from about 112 cycles/radian to about 700 cycles/radian. In terms of X_o of equation (2), where $X_o = 2\pi\nu\epsilon$ with $\epsilon = .02$ radians, then $\nu \cong 8X_o$. From equation (4) X_o will vary from 14 to 87.5. Hence $H(X_o)$ will vary from .07 to about .011. We rewrite equation (2) in the form,

$$\tau(x_o, R) = e^{-\alpha R \left[1 - \frac{S}{\alpha} H(x_o)\right]} \qquad (5)$$

For the water types considered, it can be shown that $S/\alpha \approx .2$[2]. Hence,

$$\tau(x_o, R) = e^{-\alpha R \left[1 - .2\, H(x_o)\right]} \qquad (6)$$

Substituting the values of $H(X_o)$ corresponding to focal lengths of 8mm to 50mm we have that,

$$\tau(X_o,R)_{F=8mm} = e^{-\alpha R}[1-.014] \tag{7a}$$

and

$$\tau(X_o,R)_{F=50mm} = e^{-\alpha R}[1-.0022] \tag{7b}$$

Consequently, for the waters considered and the CCD sensor considered, the MTF is independent of the scattering and the MTF for focal lengths between 8mm and 50mm is approximately,

$$\tau(R) \cong e^{-\alpha R} \tag{8}$$

At least for these conditions, the attenuation is dominant over the scattering in terms of the limiting resolution set by the CCD sensor.

B. The Effect Of Backscattering

In order to obtain an approximate estimate of the effect of backscattering on the ability of the sensor to "see" an image, a scenario is established. The scenario used for these calculations is depicted in figure 1. Here it is assumed that the center line of the light source makes an angle β with the viewing center line. The object is at the range R and z is distance from the front of the object to the edge of beam formed by the light source. A unit light source is located a distance b from the viewing axis. The light source makes a divergent beam (flash lamp) of half-angle α. From the geometry of figure 1 we have that,

$$Z = R - b\cot(\alpha+\beta) \quad \alpha+\beta < 90^\circ \tag{9}$$

At any given r, the light intensity will be reduced by,

$$\frac{e^{-\gamma r}}{r^2} \tag{10}$$

here γ is the broad beam attenuation coefficient given by $(\alpha - S)$. Each increment dr will backscatter to the viewing system according to,

$$\pi \langle \sigma_B \rangle dr \tag{11}$$

where $\langle \sigma_B \rangle$ is the average backscattering function $(90^\circ\text{-}180^\circ)$. the backscattered light travels towards the viewing systems and is further attenuated by,

$$e^{-\alpha\sqrt{r^2-b^2}} \tag{12}$$

Combining the elemental contribution produces a resultant backscattered light as,

$$dB = \frac{e^{-\gamma R}}{r^2} \cdot \pi \langle \sigma_B \rangle e^{-\alpha\sqrt{r^2-b^2}} dr \tag{13}$$

or the total contribution along the viewing direction becomes,

$$B = \pi \langle \sigma_B \rangle \int_{\sqrt{(R-Z)^2+b^2}}^{\sqrt{R^2+b^2}} \frac{e^{-\gamma r} e^{-\sqrt{r^2-b^2}}\, dr}{r^2} \tag{14}$$

This integral can only be solved numerically, hence we simplify as follows. Instead of using a variable attenuation as we go from 0 to z, we take an average attenuation factor at $\frac{z}{2}$. Hence we have that,

$$B = \frac{4\pi\langle\sigma_B\rangle e^{-\frac{\gamma z}{2}}}{z^2}\int_{R-z}^{R} e^{-\alpha r}dr \qquad (15)$$

where the integration is along the viewing axis. Although this simplifies the expression, it is believed that the result will not deviate appreciably from an exact solution. The result of integration of (15) yields,

$$B = \frac{4\pi\langle\sigma_B\rangle}{z^2}\cdot e^{-\frac{\gamma z}{2}}\cdot\frac{e^{-\alpha R}}{\alpha}\cdot\left(e^{\alpha z}-1\right) \qquad (16)$$

The signal (light scattered from the object) must be compared to the B of equation (16) to determine the effect of background.

Referring to figure 1, the attenuation of light from a unit source reaching the object will be given by,

$$S = \frac{e^{-\frac{\gamma R}{\cos\beta}}\cos^2\beta\,\rho_T}{R^2} \qquad (17)$$

where ρ_T = object diffuse reflectivity. In this derivation, it is assumed that the background scattered light can be considered as part of the object background (i.e. reduction in object contrast).

In order to use equations (16) and (17) we define the optical meaning of contrast as various authors use different expressions for contrast. In terms of MTF, contrast is modulation defined by,

$$C = \frac{I_{MAX} - I_{MIN}}{I_{MAX} + I_{MIN}} \tag{18}$$

where I_{MAX} and I_{MIN} stand for maximum and minimum intensity respectively. With this definition of contrast we can write that,

$$C = \frac{(S+B) - B}{(S+B) + B} \tag{19}$$

or

$$C = \frac{S}{S+2B} \tag{20}$$

Rewriting we have that,

$$C = \frac{1}{1 + \frac{2B}{S}} \tag{21}$$

The term 2B/S, substituting from equations (16) and (17) becomes

$$\frac{2B}{S} = \frac{R^2}{Z^2} \cdot \frac{8\pi \langle \sigma_B \rangle}{\alpha} \cdot \frac{e^{-\gamma\left[\frac{Z}{2} - \frac{R}{\cos\beta}\right]} e^{-\alpha R}\left(e^{\alpha Z} - 1\right)}{\cos^2\beta \, \rho_T} \tag{22}$$

This expression, combined with equation (21) will yield the reduction in object contrast due to backscattering.

It is noted that the expression (22) is an approximation and may fail under certain conditions. Even with the approximations made, we still have a fairly complicated expression.

III. Water Types Considered

For this analysis, we have considered three water types which are characteristic of:

(1) clear ocean surface waters - Type I (BAHAMAS AND TONGUE OF OCEAN)

(2) coastal waters - Type II (CALIFORNIA)

(3) bay waters - Type III (CALIFORNIA)

The characteristics of these three types of waters are given in table I. This table was compiled from data obtained from references (2) and (3).

TABLE I. Optical Parameters Of Three Water Types

Type	α (Meter^{-1})	$S_{1.1^\circ}$ (Meter^{-1})	$\frac{S_{1.1^\circ}}{\alpha}$	$\langle \sigma_B \rangle$ (Meter^{-1} Ster.$^{-1}$)	$\frac{\langle \sigma_B \rangle}{\alpha}$ (Steradian^{-1})
I (Surface - Ocean)	.199	.0417	.2095	6.1×10^{-4}	3.065×10^{-3}
II (Off-Shore)	.470 .398	.103 .077	.219 .193	7.8×10^{-4} 5.8×10^{-4}	1.66×10^{-3} 1.46×10^{-3}
III (Bay)	1.92 2.19	.366 .422	.191 .193	6.1×10^{-3} 7.4×10^{-3}	3.38×10^{-3} 3.31×10^{-3}

For the calculations we have rounded off the values for simplification and have used the following parameters:

	α	$S_{1.1^\circ}$	$\frac{S_{1.1^\circ}}{\alpha}$	$\frac{\langle \sigma_B \rangle}{\alpha}$
TYPE I:	.20	.04	.20	3.0×10^{-3}
TYPE II:	.40	.10	.20	1.5×10^{-3}
TYPE III:	2.00	.40	.20	3.0×10^{-3}

IV. Sensor Considerations

In order to calculate the image reduction in contrast due to the various factors we note that the MTF is related to object and image contrast by,

$$C_i(\omega,R) = \tau(\omega,R)C_o(\omega,R) \tag{23}$$

where C_i = resultant image contrast

C_o = object contrast

Substituting for object contrast in the presence of backscattering, we have that,

$$C_i = \tau\left[\frac{1}{1+\frac{2B}{S}}\right] \tag{24}$$

Substituting for τ from equation (8) we have that,

$$C_i = e^{-\alpha R}\left[\frac{1}{1+\frac{2B}{S}}\right] \tag{25}$$

However, the threshold contrast that can be measured by the sensor (limited by noise) will determine the lower limit of C_i. For the CCD at 14 cycles/mm, the contrast is approximately 50%. Consequently,

$$C_t = C_i \cdot C_s \tag{26}$$

Where C_t is the threshold contrast and C_s the sensor contrast. For high levels of illumination, a reasonable value for C_t=.02. With C_s=.50 we have that the limiting image contrast that can be obtained is about .04 at 14 cycles/mm. Consequently, for each water type there

is a limiting range for which C_i is .04. Rather than just calculating this range, we have chosen to plot the image contrast as a function of R for each water type and only indicate on each graph the value corresponding to C_t=.02. The reason for depicting the results this way is that C_t will depend a great deal on the level of illumination and the curves can be used to determine R at any value of C_t. The results of this analysis is depicted in figures 2, 3, and 4 for three different values of b and a range of object reflectivities from .2 to 1.00.

V. Conclusions

For a broad beam light source (i.e. a flash lamp with a half-angle divergence α of about 30°) and utilizing a CCD sensor with a limiting resolution of 14 cycles/mm at 50% contrast, the results of this analysis yields the following information:

(1) In going from water type I to III, the effect of target reflectivity becomes less important as the figures indicate on image contrast.

(2) The distance between light source and viewing system b, does not affect the contrast calculations appreciably. In fact, the figures indicate separating the light source from the viewing system produces a lower contrast in the image. This is somewhat unexpected, but is due to the greater attenuation, as b increases, resulting in less energy density at the target plane.

(3) If we assume that the lowest contrast measurable is .02, then we have the following values for range (indicated by dashed line in the figures):

TYPE I (b=O)

ρ_T	RANGE (Meters)
no scattering	~16
1.00	~15
.60	~14.5
.40	~14.0
.20	~12.5

TYPE II (b=O)

ρ_T	RANGE (Meters)
no scattering	8.0
1.00	7.6
.20	7.0

TYPE III (b=O)

ρ_T	RANGE (Meters)
no scattering	1.6
.20	1.2

For the other values of b, the results are correspondly lower in range. For other values of threshold contrast, the range values

would be correspondingly lower or higher. For example, if the threshold contrast were .05 instead of .02, the image contrast necessary would be C_i=.10 (.05/.5). From figure 2, the ranges would vary from:

TYPE I: 11.4 to 9.0 for ρ_T to .20

TYPE II: 5.7 to 5.0 for ρ_T to .20

TYPE III: 1.2 to 0.8 for ρ_T to .20

Again the values for higher b values would be correspondingly lower and can be obtained from figures 3 and 4.

References

(1) H. SADJIAN, "Parameters That Govern Image Quality And Pattern Recognition Techniques For Underwater Optical Imaging"; General Sensors, Inc., Report GS-ONR-2-1978; prepared for the U.S. Geological Survey, Reston, Virginia, 30 November 1978. AD A063617.

(2) T.J. PETZOLD, "Volume Scattering Functions For Selected Ocean Waters", University of California, San Diego, California, S10 Reference 72-78, October, 1972; prepared for the Naval Air Development Center, Warminster, Pa.

(3) E.J. SOFTLEY and J.F. DILLEY, "In Site Measurements Of Small And Large Angle Volume Scattering Of Light In The Sea", Ocean and Atmospheric Sciences Laboratory, General Electric Co.; presented at the 1972 IEEE Conference On Engineering In The Ocean Environment, Newport, Rhode Island, Sept., 1972.

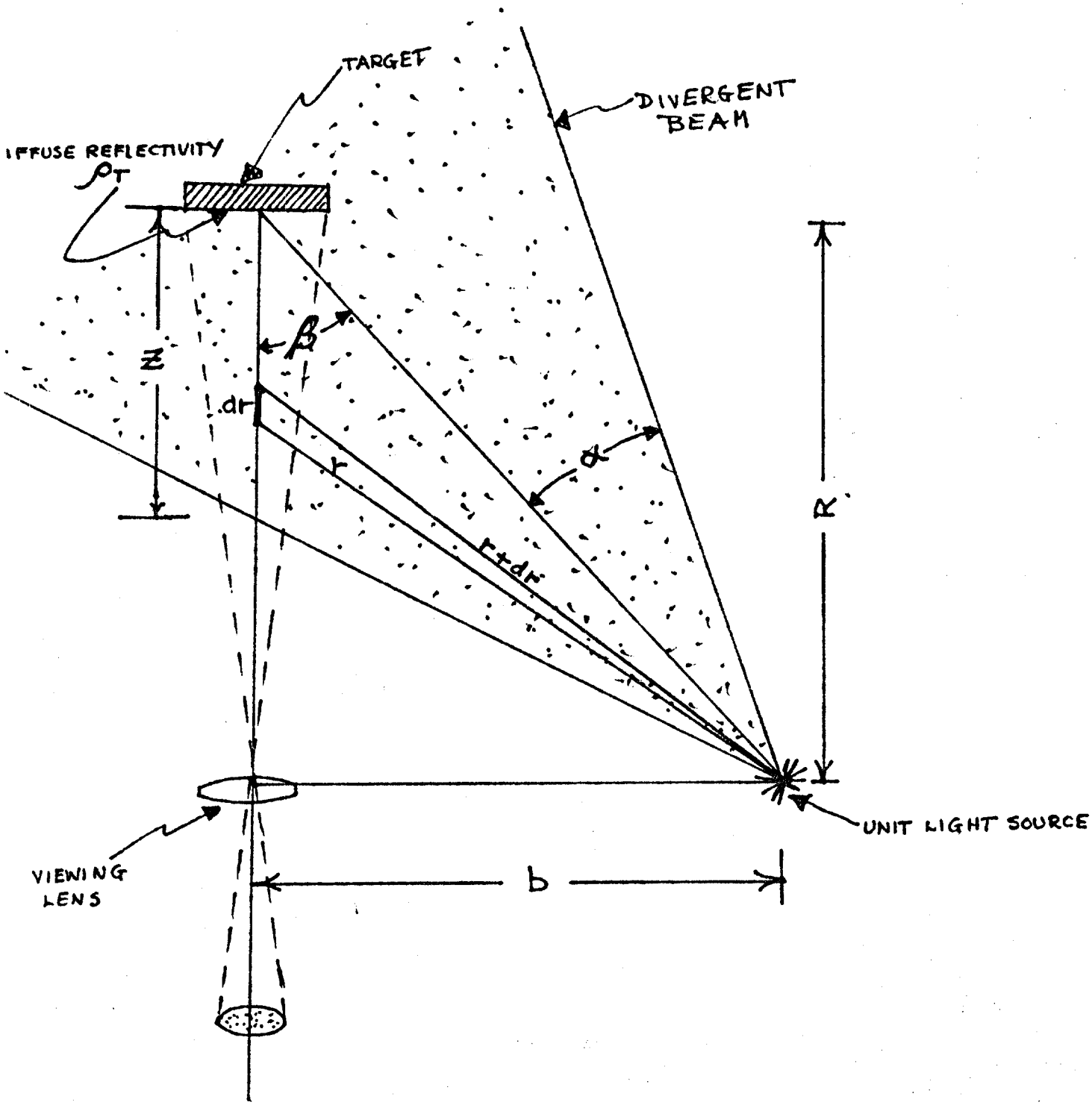

Figure 1. Geometry Used To Derive The Backscattering Equations. See Text.

Figure 2. Image Contrast With And Without Backscattering For b=0. See V.

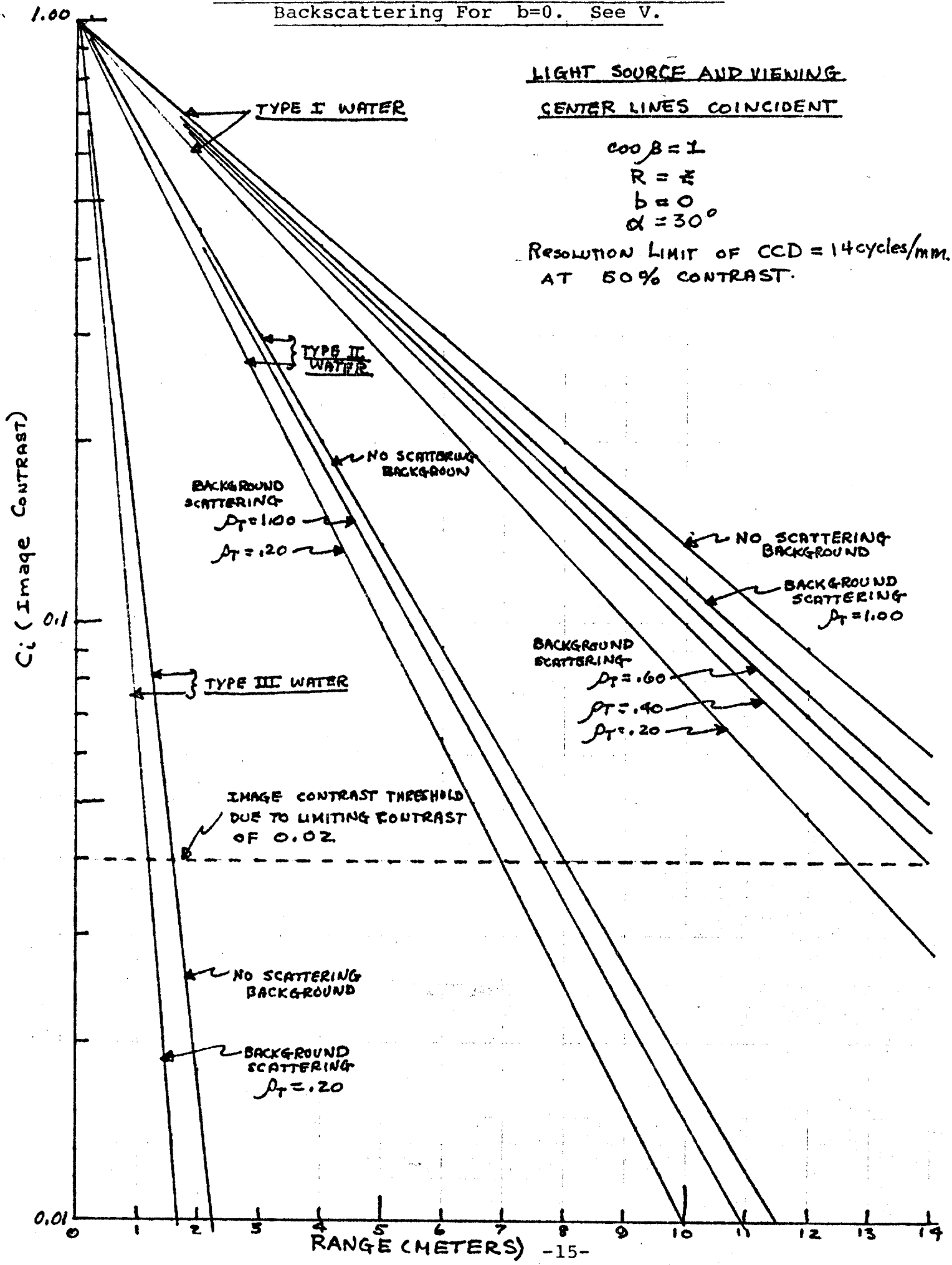

Figure 3. Image Contrast With And Without Backscattering For b=0.1R. See V.

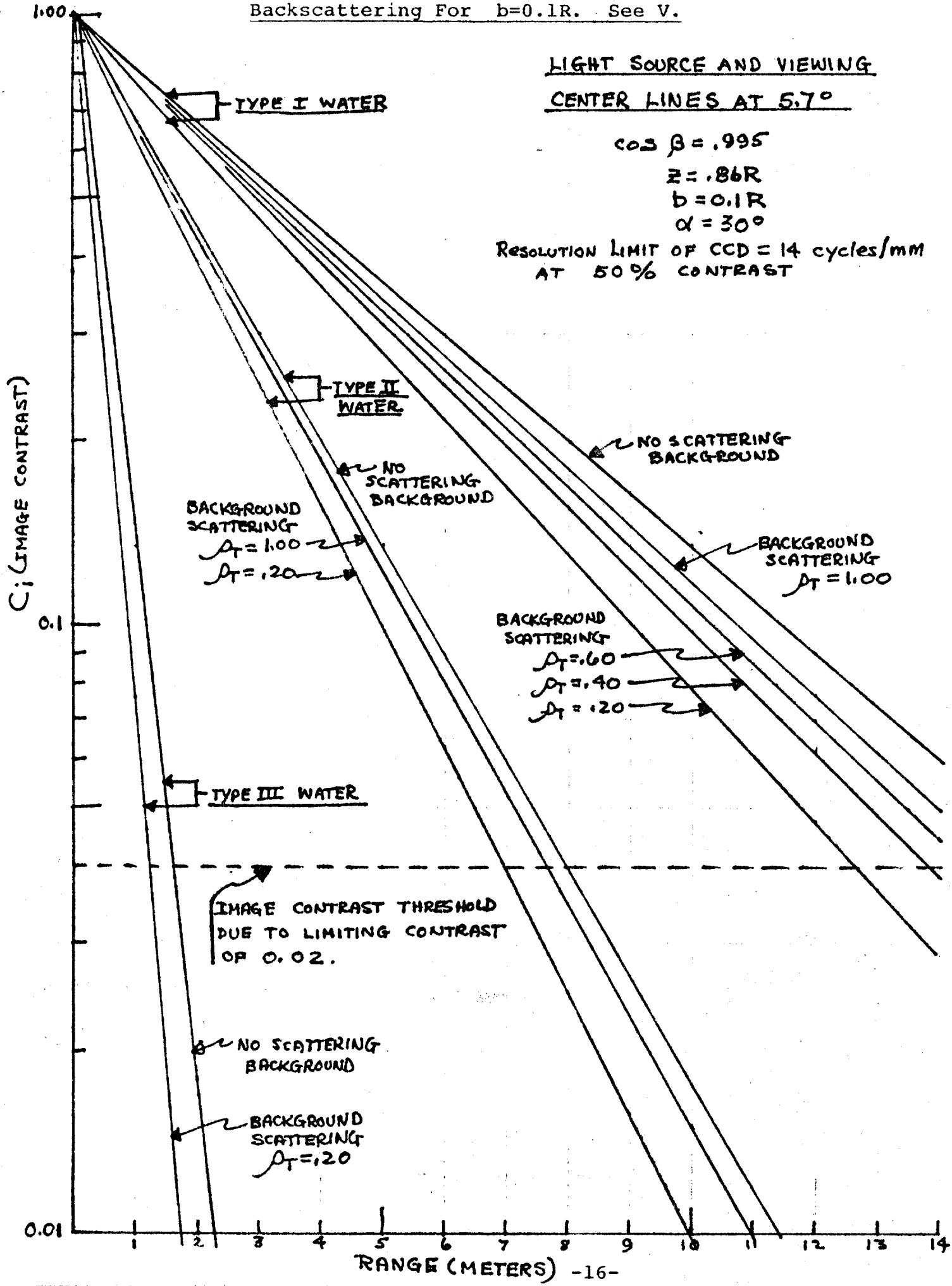

Figure 4. Image Contrast With And Without Backscattering For b=0.5R. See V.

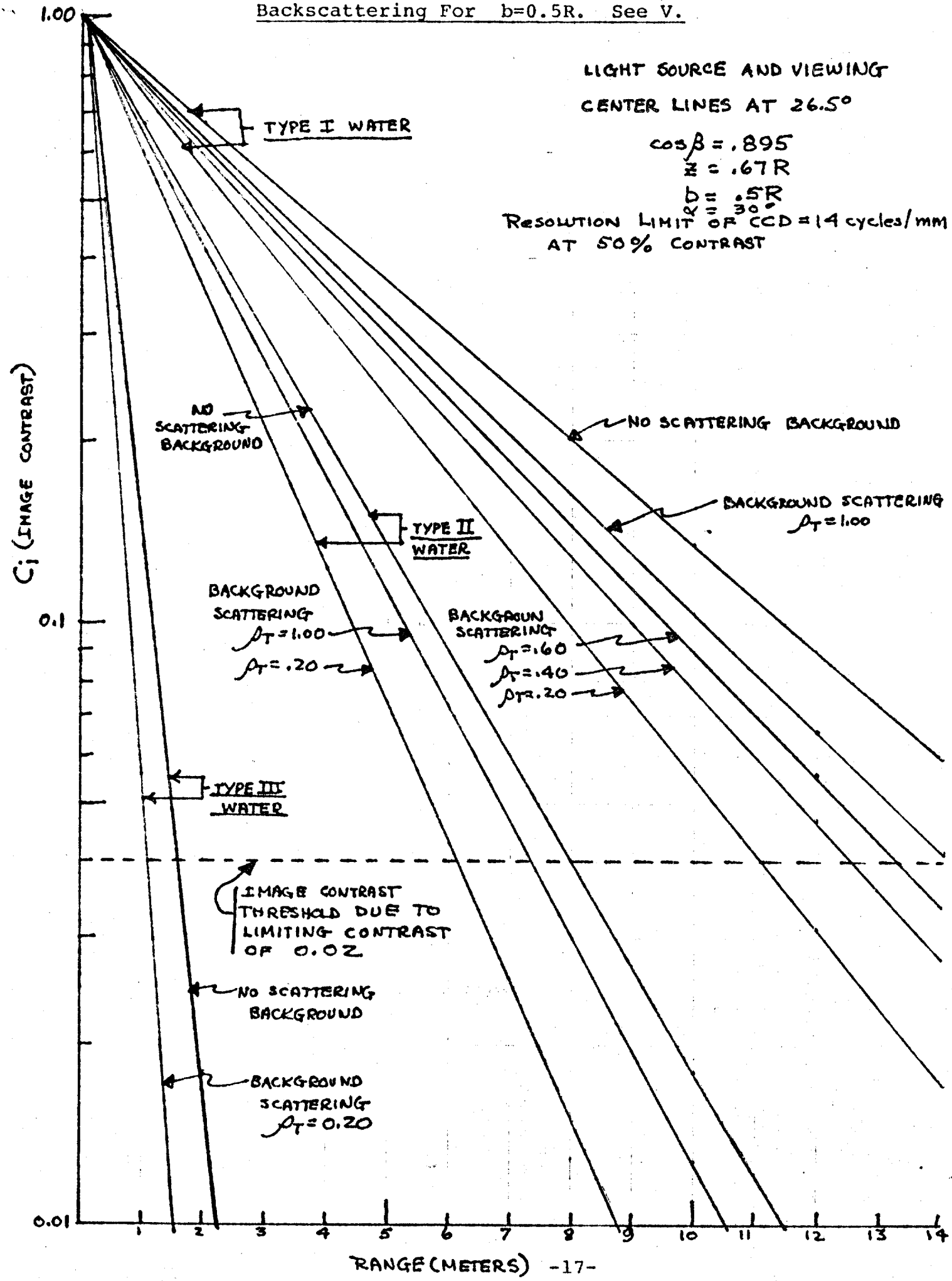

The Reticon RA100x100 is a two-dimensional self-scanned optical sensor array with optimized characteristics. 10,000 discrete photodiodes are geometrically arranged into a 100x100 matrix. In contrast to comparable CCD devices, the discrete photodiode sensors require no surface electrode so that there is no interference pattern or light loss and the full inherent sensitivity is obtainable.

The scanning method permits pixel rates up to 10 MHz. Each line of pixel information is parallel loaded into high-speed bucket-brigade analog shift registers and sequentially shifted out. All 100 lines may be sequentially accessed to give a 100-line frame, or alternate odd or even lines may be selected to produce 50 lines per field in an odd and even field pattern. These fields may be interlaced, or each may be used singly in a frame. .The integration time is nominally one frame period, giving maximum sensitivity.

FEATURES

- 10,000 light-sensitive elements in a high-resolution 100x100 matrix.
- 60 µm center-to-center element spacing in both X and Y directions.
- Frame storage - each diode integrates photocurrent for the entire frame.
- Self-scanned in both X and Y directions by high-speed on-chip circuitry to provide either single frame or interlaced odd/even field multiplexed serial video output.
- Non-burning sensors.
- Solid-state reliability.
- Low power dissipation.
- 24-pin dual-in-line package (1.2 inch x 0.6 inch) with scratch-resistant quartz window.

GENERAL DESCRIPTION

The RA100x100 is packaged in a 24-pin dual-in-line package with a ground and polished window covering the mask-defined active area. Figure 1 is a diagram of the device which also shows its connection diagram. The device, fabricated on a monolithic silicon chip, contains the matrix diode array with access and reset switches in addition to both the X and Y read-out shift registers. Figure 2 is a schematic representation.

7-7-80

EG&G RETICON • 345 POTRERO AVENUE • SUNNYVALE, CALIFORNIA 94086
TELEPHONE: (408) 738-4266 • TWX 910-339-9343

EG&G RETICON PRELIMINARY DATA SHEET
SOLID-STATE IMAGE SENSOR ARRAY RA100x100

A MOS dynamic shift register sequentially selects the diode row in the matrix while the selected diode from each column of diodes is accessed via a parallel transfer gate which controls the parallel transfer of charge into two bucket-brigade shift registers. These registers are clocked such that they allow the transfer to the output of the information from the diode row after each Y register shift. The sequence thus is: select the row, Y; transfer the row's information to the X register and reset the diodes; readout the pixel information in the X direction while advancing the Y or row selection.

One bucket brigade obtains information from odd and the other bucket brigade the information from even diode columns and each then shifts that information sequentially to the output. The even video is shifted an extra 1/2 cycle of the shift frequency, ϕ_{X1}, to obtain the desired time sequence. The alternating odd and even signals are then transferred to corresponding output ports video 1 and video 2.

Two controls are used to control integration time and field/frame sequence. A special frame reset permits resetting all photodiodes simultaneously, if desired. A field control permits selection of odd lines only, even lines only, odd and even lines in sequence, or an odd field followed by an even field in an interlace mode.

INPUT/OUTPUT DEFINITIONS AND FUNCTIONAL DESCRIPTION

The matrix array has functional elements which serve to control the timing sequences for diode access, to transport the pixel information to the output, to control integration time, to control the odd and even fields, to provide for interlace, and to buffer each video output. The external circuit provides the timing and the bias to these functional elements as well as clocks to control LO, LE, LR, LT, V_{BUFF}, Y_{START}, EOF, FR, VR_1, VR_2, VQ_1 and VQ_2.

1. The Odd and Even Bucket-Brigade Transports and their Clocks, ϕ_1-ϕ_2.

Figure 2 shows two bucket-brigade analog shift registers which are located on either side of the device. These are the odd and even transport registers which accept the pixel information in parallel from their respective odd and even video diode columns and shift the pixel information sequentially to the output amplifier. Each bucket brigade must be provided with a two-phase clock as shown in Figure 3. Note: To insure high transfer efficiency, it is important that the clock waveforms cross at or below the 50% level. Normally these clocks swing from a low of 0.4 volts to a high of 15 volts. Again, as evident from Figures 2 and 4, the transfer into both shift registers takes place simultaneously during the time ϕ_{X2} is held high. However, on read out, the odd bucket brigade produces the first pixel, since it reads out on the first low-going ϕ_{X2} clock just after the transfer period. The second pixel is produced by the even shift register, because this pixel must transfer through an extra half-stage which is controlled by ϕ_{X1} clock; thus when ϕ_{X1} goes low the even pixel is produced to provide an easily multiplexed signal by means of a simple adder amplifier. Furthermore, the multiplexing increases the pixel rate to 2 times the transport clock frequency. See Figure 4 for the clock timing diagram.

2. The Y Dynamic Shift Register

This shift register is shown in Figure 2 as a block with 100 outputs, each connected to a row of photodiode access switches. When the shift register is clocked, each row is sequentially activated, thus sequentially connecting a row of diodes to the column video lines that provide paths for the diode information to the bucket brigade via the line transfer switch. Tied to each output of the shift register (except for the 100th position) are inputs to a nor gate which provides for the self-loading feature. When there is an output from any of the 99 output positions the nor gate keeps the shift register from loading. Once the bit occupies the last position the nor gate's output goes high and the shift register loads with the rising edge of ϕ_{Y1}. Note that Y_{START} is connected to the nor gate. It can be used to inhibit the register from loading by pulling Y_{START} to V_{DD}. The register requires a two-phase clock which typically swings from a low of 0.4 volt to V_{DD}. Odd lines are accessed while ϕ_{Y1} clocks are high, even while ϕ_{Y2} is high.

3. Line Select Controls, LO and LE

As evident from the schematic diagram, Figure 2, the LO input terminal controls the gates that switch all of the odd-numbered outputs from the Y shift register; the LE terminal controls the gates that switch the even-numbered outputs. These Y-register outputs in turn control the row selection. When the LO line is held at V_{DD}, the odd rows of diodes may be selected by the Y shift register; when the LE line is held at V_{DD}, even rows of diodes may be selected. The selected diodes are connected to the column output lines which, in turn, are connected to transport bucket brigades through buffer transistors and the line transfer switches. Typically, the LO or LE terminal when selected is switched from a low of 0.4 volt to a high of V_{DD}. For sequential scan of all 100 lines, both LE and LO are continuously held at V_{DD}.

4. Line Reset, LR

This input is normally clocked in synchronism with ϕ_{X1}. However, to avoid crosstalk and to permit an adjustment for optimum blooming control, a separate driver is used for LR. An active LR maintains the potential of the column video lines between line transfers and hence bleeds off excess charges, collected under excess illumination, that would otherwise add to blooming. See section on Very High Speed Operation.

5. Line Transfer, LT, and Line Buffer, V_{BUFF}

The LT pulse input controls the period during which the row of diode information is transferred into the bucket-brigade transport registers. This pulse must occur while LR is off (low). Normally this LT input is clocked as seen in Figure 5 with rise and fall as in the electrical specifications. The line buffer control, V_{BUFF}, is normally held at approximately 0.8 V_{DD} and adjusted to optimize blooming control. However, its level becomes critical to input-output linearity in the high-speed mode; under those conditions it is set at or near +8.8 volts.

6. Y Shift Register Start, Y_{START}

The Y_{START} input provides access to one of the inputs to the Y shift register's nor gate as seen in the schematic diagram, Figure 2. When this input is held high, the output of the nor gate is held low and inhibits loading of the shift register; however, when the Y_{START} input is pulled low, the nor output rises (after line 100 is accessed) and a bit is loaded into the register with the rising edge of ϕ_{Y1} clock. The first row is then immediately accessed when ϕ_{Y1} rises.

7. End of Frame, $\overline{EOF}$

As discussed under Y_{START}, the Y shift register has a nor gate which provides control for the self-starting feature. The nor gate output is connected to an external pin through an open-drain inverter. This output is normally tied to V_{DD} through an 8.6K resistor; therefore, when there is a bit in any row except the last or if Y_{START} is active $\overline{EOF}$ will remain high. It goes immediately low on the rising edge of ϕ_{Y2} if Y_{START} is low and none of the rows 1-99 are active. This point will sink a maximum of 1.5 ma.

8. Frame Reset, FR

This input controls access switches to every diode in the matrix and provides simultaneous refreshing of all diodes. Since the diodes in each line are automatically reset when the line is accessed, the frame reset control is not normally used and is held low. However, when a particular exposure is desired, this control may be used to clear the diodes to start a fresh integration cycle by taking the FR terminal to V_{DD}. When this mode is used a shutter or pulsed light input is required because the diodes are sequentially accessed and will thus differ in exposure time if light input is continued during the read-out sequence.

9. Reset Clocks for the Gated-Charge Amplifiers, V_{R1} and V_{R2}

These terminals provide reset voltages for the gated-charge amplifiers which are shown in the schematic diagram, Figure 2, at the outputs of both bucket brigades. On the even side, the signal appears at the gate of the output source follower when ϕ_{X1} drops to a low potential. While ϕ_{X1} is high before the next sample appears this node is cleared by charging it to a reset voltage, R_D. Reset thus is accomplished when this terminal is clocked synchronously with ϕ_{X1}. The complementary situation applies to the odd output, with signal appearing while ϕ_{X2} is low and reset while ϕ_{X2} is high. The extra half-stage in the even side allows the alternating sequence desired. Normally, the synchronous relationship is obtained by direct connection of ϕ_{X1} to V_{R2}, and direct connection of ϕ_{X2} to V_{R1}.

10. Video Output Terminals, VID_1 and VID_2

The video output is that of a source follower. Normally, the output of each source follower is connected to 2K Ω which is referenced to ground. This configuration provides the proper bias current for the source follower. Figure 5 shows the output voltage across such a load resistor, showing the relationship of the video pixel information relative to the superimposed reset clock amplitude.

Figure 6 shows the output impedance of the source follower as a function of the bias current. This graph can be used to design a desired interface circuit with suitable dc bias translation (e.g., an emitter-coupled transistor with the base biased up near the video output line potential).

11. Input Bias, VQ_1 and VQ_2

Bias inputs are connected to current ports at the bias inputs of both bucket-brigade transports, VQ_1 to the odd and VQ_2 to the even. These inputs control the bias level in the dark. Nominally, these terminals are biased to approximately 4 volts; however, when the odd and even videos are summed together either input bias voltage may be used to adjust the corresponding dark-level output to remove the odd-and-even pattern.

OPTIMUM CLOCK AND BIAS RELATIONSHIPS

Optimum performance from the device is normally obtained with the ϕ_{X2} and LT clocks interleaved as shown in Figure 4 and with LR clocked with ϕ_{X1}. In this mode of operation the optical to electrical transfer function is given in Figure 7. The dynamic range is in excess of 100:1 with a noise-equivalent exposure of less than 1.5×10^{-9} joules/cm^2.

The important relationships which must be observed are timing of the clock transitions of ϕ_{X1}, ϕ_{X2}, ϕ_{Y1}, and ϕ_{Y2}; the zero level of LT; and the relative timing relationship between LT and ϕ_{X2}.

ϕ_{X1} and ϕ_{X2} are complementary clocks with crossover of the transition edges taking place below 50% of the clock amplitude. Rise and fall times preferably are in the order of 20 nanoseconds. This edge control is required to obtain the optimum efficiency from the bucket-brigade transport.

ϕ_{Y1} and ϕ_{Y2} also are complementary and should cross below the 50% level at the transition edges and should have rise and fall times in the order of 40 nanoseconds.

The transition-edge spacing of the interleaving clocks LT and ϕ_{X2} should be kept as shown in the detailed timing diagram of Figure 4.

VERY HIGH SPEED OPERATION

In most applications, the above described normal mode is preferred. However, the interleaved clock relationships do not permit operation above approximately 5MHz sample rate. An alternate high-speed mode may become preferable when speed requirements are dominant. For this mode, however, careful attention must be paid to timing, V_{BUFF} becomes critical to the maintenance of linearity, and blooming control is less effective.

For the high-speed mode, the timing relationships are shown in Figure 8, and the critical V_{BUFF} potential becomes 8.8 volts instead of a level near the V_{DD}. The transfer characteristic degrades in linearity and the dynamic range is reduced. The primary operation changes lie in the relationships between LT and ϕ_{X2}, in the critical setting of V_{BUFF}, and in the changes in the pulse drive of LR.

ELECTRICAL SPECIFICATIONS

Table I lists the major sensitivity specifications and Table II the operating biases and clock amplitudes in accordance with the timing diagram of Figure 4.

With the exception of the supply inputs such as V_{DD}, the input impedances to the input terminals are essentially all capacitive. The capacitances are listed in Table III.

OPTICAL TO ELECTRICAL PERFORMANCE

The circuit which has been used to obtain the following typical performance characteristics is essentially identical to the evaluation circuit offered by Reticon under the designation RC-502 (a schematic diagram is shown in Figure 11); however, the video processing circuit there shown has not been used. Instead, all measurements have been taken across a 2K load to ground.

The optical source for the performance data is a 2870°K tungsten source. Illumination levels are measured using a detector with a flat response from 370 to 1040 nm.

Spectral Response and Transfer Function

The spectral response is the standard silicon photodiode response as shown in Figure 9. In contrast with CCD detector arrays, there is no semitransparent electrode covering the sensors and hence no interference patterns in the pass band and no additional attenuation at short wavelengths.

The transfer function (Figure 7) shows a linear optical-to-electrical relationship with dynamic range exceeding 100:1. This linear relationship is dependent on application of the proper electrode potentials, especially those for V_{BUFF} and the line reset pulse level, LR. Improper potentials can cause substantial non-linearity.

Anti-Blooming

Blooming is generally less severe in the RA100x100 type of structure as compared to typical CCD structures because the RA100x100 sensor elements are separate and distinct PN junction photodiodes; however, since there are common video lines for each column of diodes, a vertical-blooming effect is observed since some excess charge is collected on the column video line. Blooming is defined, here, as the ratio of the excess charge integrated on the column video line per sample period (as a result of excess exposure of a group of photodiodes) to the amount of excess exposure.

Figure 10 is a curve of this ratio; i.e., points on the horizontal axis represent multiples of saturation exposure and points on the vertical axis represent the output of a non-exposed diode locate 15 diodes away from the exposure center but sharing the same column video line. The output is normalized to the output voltage of a saturated diode and plotted in percent of the saturation voltage. The exposed area is circular with a diameter of approximately 10 diodes.

ARRAY MECHANICAL CHARACTERISTICS

		Units
Number of Diodes	10,000	
Diode X, Y center to center spacing.	60/2.36	μm/mils
Diode sensing area	2.1×10^{-5}	cm^2
Package size (24 pin)	.6 x 1.2	inch

TABLE 1

ARRAY PERFORMANCE CHARACTERISTICS ($T_A = 25^\circ C$)

SYMBOL	PARAMETER	MIN.	TYP.	MAX.	UNITS	NOTES
DR	Dynamic Range (P-P)		100:1		-	1
E_{NE}	Peak-To-Peak Noise Equivalent Exposure		1.5×10^{-3}		$\mu j/cm^c$	
E_{SAT}	Saturation Exposure		0.2		$\mu j/cm^2$	
R	Responsivity		10		$V per \mu j/cm^2$	
	Photoresponse Non-Uniformity		±10	±15	%	
V_{DARK}	Average Dark Signal		1	2	%	2
V_{SAT}	Saturation Output Voltage		2		V	3
R_O	Output Impedance		2K		Ohms	
FS	Video Sample Rate			10MHz		4

1. Ignoring lines 1, 2 and 100
2. Integration time 40ms. Dark signal changes by a factor of 2 every 7° C.
3. Voltage measured across 2KΩ load resistor.
4. Odd and even video outputs combined.

TABLE 2

RA 100 X 100 AREA ARRAY SPECIFICATION SHEET

Definition	Symbol	Parameter			Dimension
		Min.	Typical	Max.	
X Direction Transport Shift Reg.	ϕ_{X1}	12	V_{DD} - 0.5	V_{DD}	Volt Peak *
	ϕ_{X2}	12	V_{DD} - 0.5	V_{DD}	Volt Peak *
Y Direction Digital Shift Reg.	ϕ_{Y1}	12	V_{DD} - 0.5	V_{DD}	Volts Peak *
	ϕ_{Y2}	12	V_{DD} - 0.5	V_{DD}	Volts Peak *
Y Shift Reg. Reset	Y_{START}	12	V_{DD} - 0.5	V_{DD}	Volts Peak □
Line Transfer	LT	12	V_{DD} - 0.5	V_{DD}	Volts Peak □
Line Reset	LR	0	0	V_{DD}	
X Transport Input Bias Odd	VQ1		4 Volts		Volts D.C. □
X Transport Input Bias Even	VQ2		4 Volts		Volts D.C. □
Video Reset 1 (Odd)	VR_1		V_{DD} - 0.5	V_{DD}	Volts D.C.
Video Reset 2 (Even)	VR_2		V_{DD} - 0.5	V_{DD}	Volts D.C.
Reset Drain	RD	10.5	V_{DD} - 1.5	V_{DD} - 1.5	Volts D.C.
Reset Drain Current	RDI	3	6	9	μamp
Frame Reset	FR		V_{DD} - 0.5	V_{DD}	Volt Peak
Isolation Gate	V_{BUFF}	V_{DD} - 1.7	V_{DD} - 1.5	V_{DD}	Volts D.C.
DC Supply	V_{DD}	12	15	17	Volts D.C.
DC Current	I_{DD}	6	8	10	ma
X Transport Tetrode Gate Bias	V_{BB}	11	ϕ_X-0.5	16	Volts D.C.
Odd Line Switch	LO	12	V_{DD} - 0.5	V_{DD}	Volts Peak □
Even Line Switch	LE	12	V_{DD} - 0.5	V_{DD}	Volts Peak □
End of Frame	$\overline{EOF}$	—	—	—	Volts □

NOTE: * All voltages measured with reference to common (ground)

□ See text.

TABLE 3

ELECTRICAL SPECIFICATIONS

TYPICAL CAPACITANCE WITH 10 VOLTS BIAS

PIN	SYMBOL	CAPACITANCE	UNITS
2	$\overline{EOF}$	5	pf
3	LO	19	pf
4	LE	18	pf
5	LR	17	pf
7	VR_1	4	pf
8	ϕ_{X1}	44	pf
9	ϕ_{X2}	44	pf
10	FR	12	pf
12	VID_1	5	pf
13	VID_2	5	pf
16	ϕ_{X2}	44	pf
17	ϕ_{X1}	44	pf
18	VR_2	4	pf
21	LT	18	pf
22	Y_{START}	4	pf
23	ϕ_{Y1}	25	pf
24	ϕ_{Y2}	25	pf

TABLE 4

TERMINAL INPUT CAPACITANCE

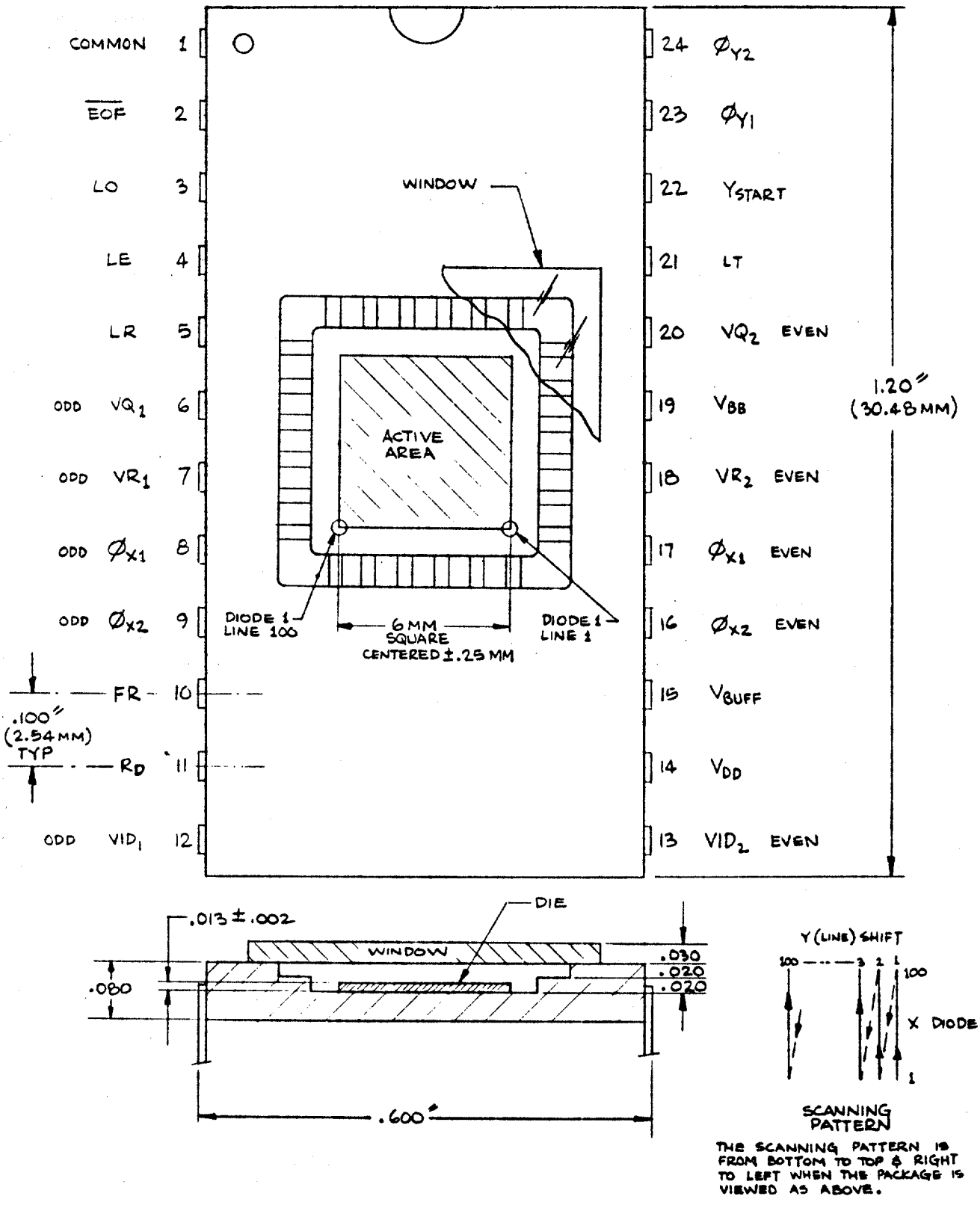

FIGURE 1 — RA 100 × 100 PACKAGE AND PIN CONFIGURATION

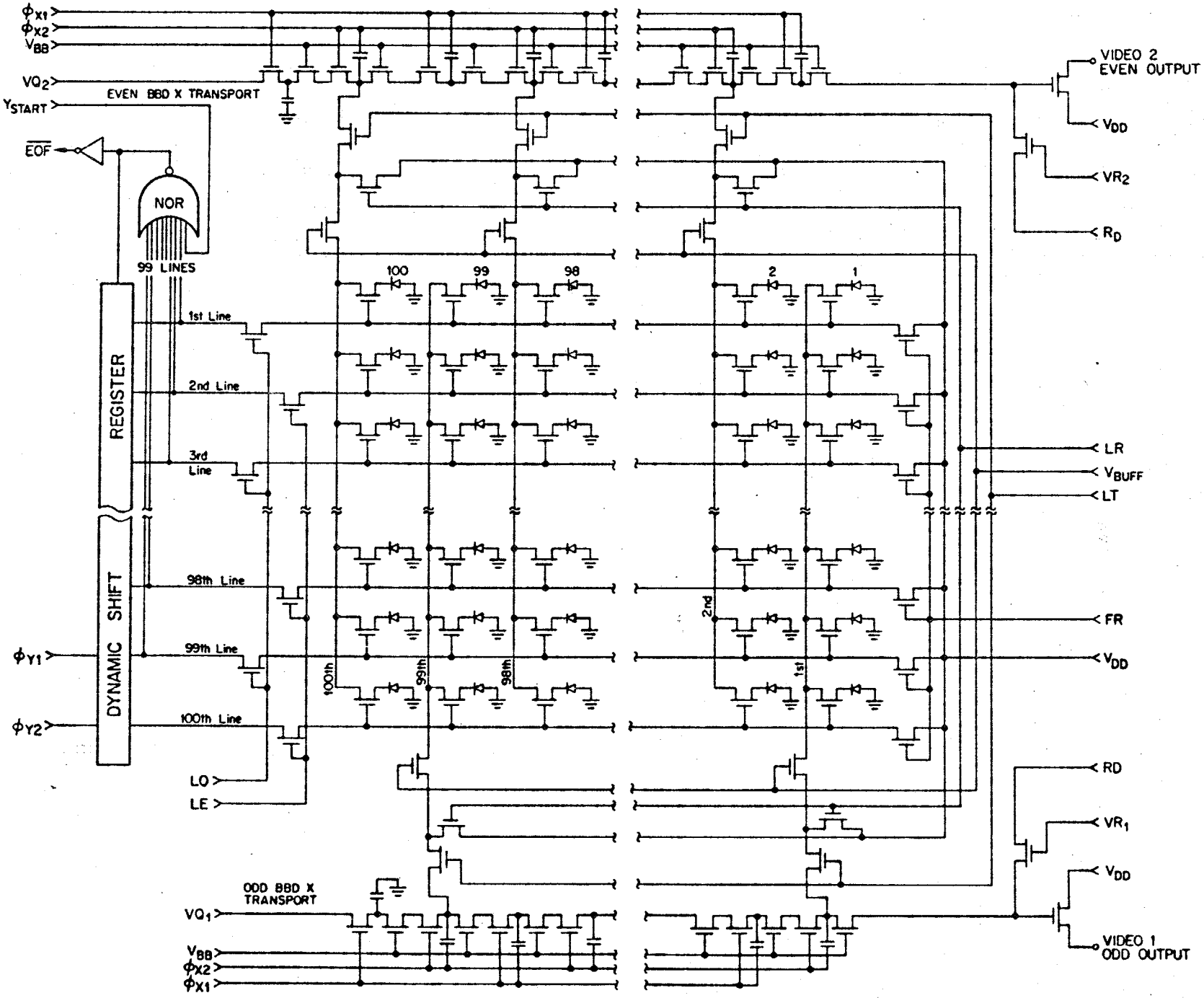

FIGURE 2 - Schematic Diagram, RA 100x100

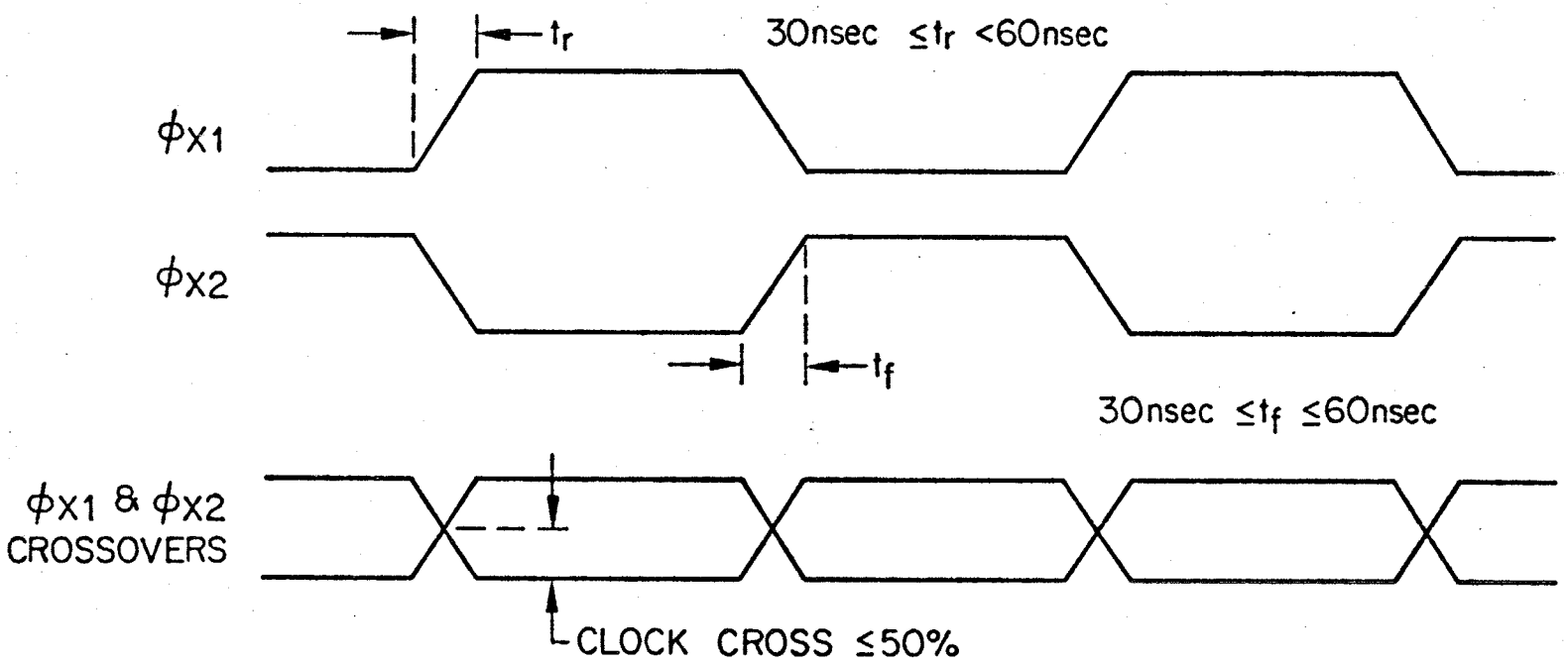

FIGURE 3 - $\emptyset_{X1}$ and $\emptyset_{X2}$ Clock Shapes

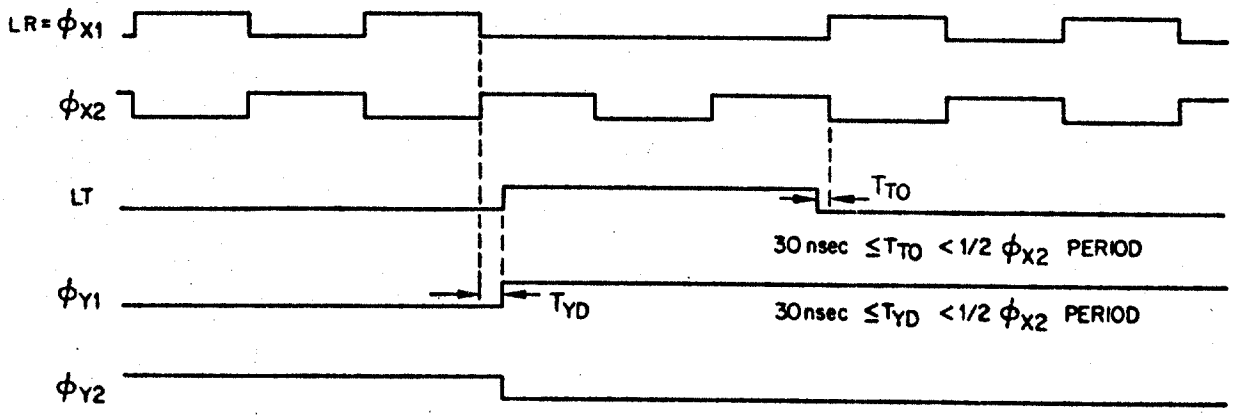

FIGURE 4 - Clock Operation Timing Diagram

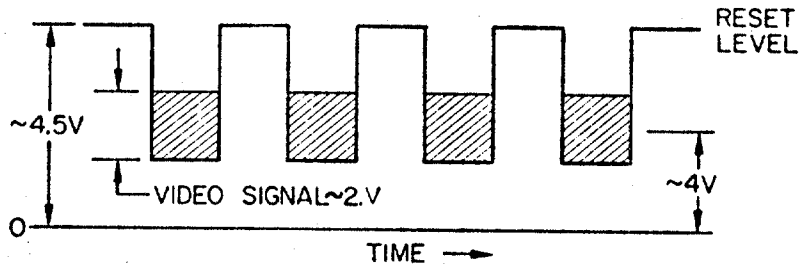

FIGURE 5 - Typical Video Signal Seen Across 2K Ω

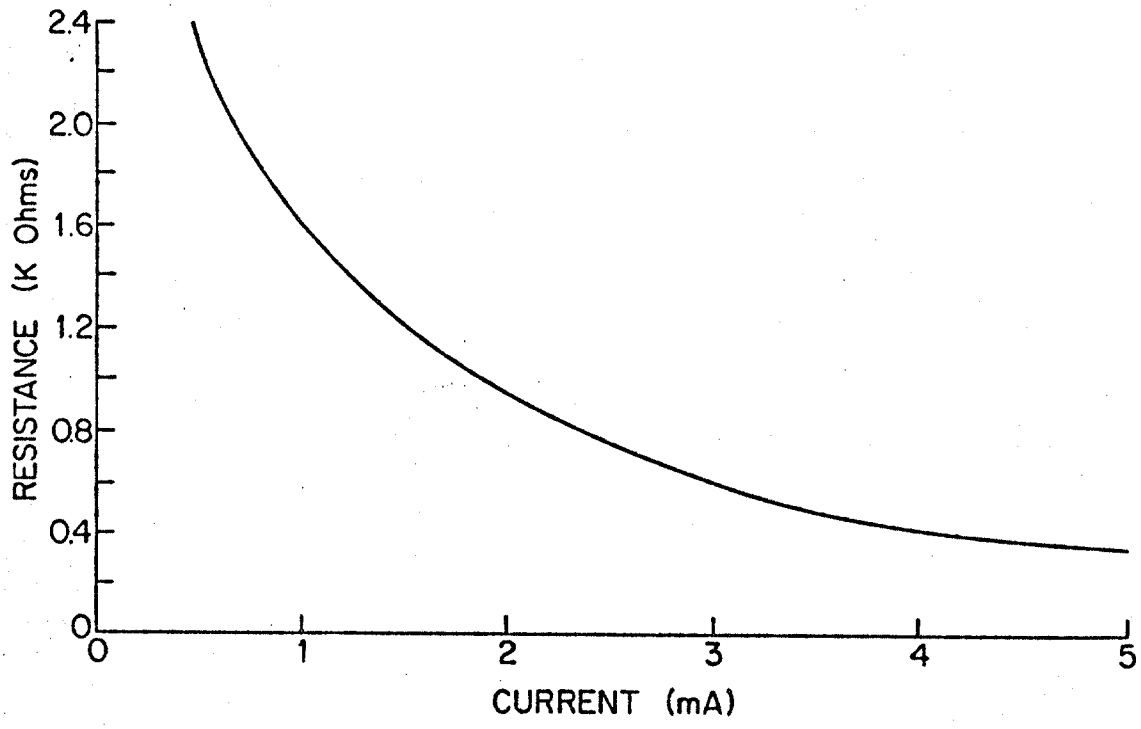

Figure 6 - Typical Video Output Impedance vs. Bias Current.

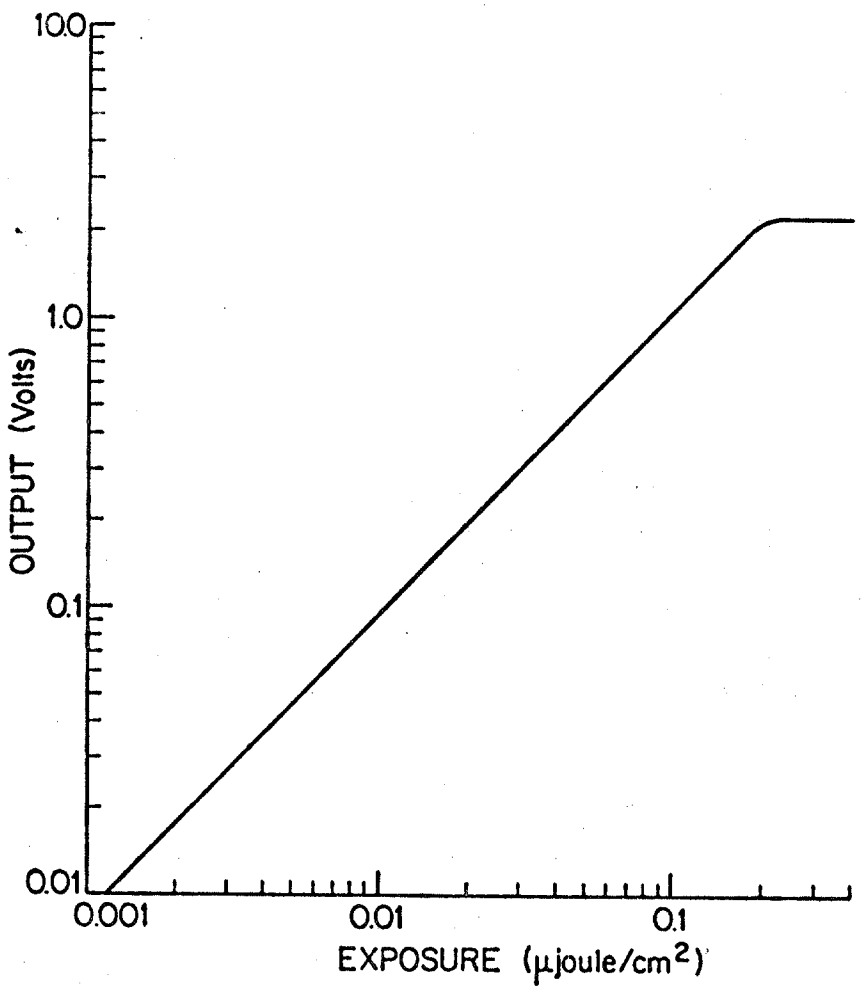

Figure 7 - Output vs. Exposure (2870° K tungsten source measured using a detector with flat response and 370 to 1040nm bandwidth).

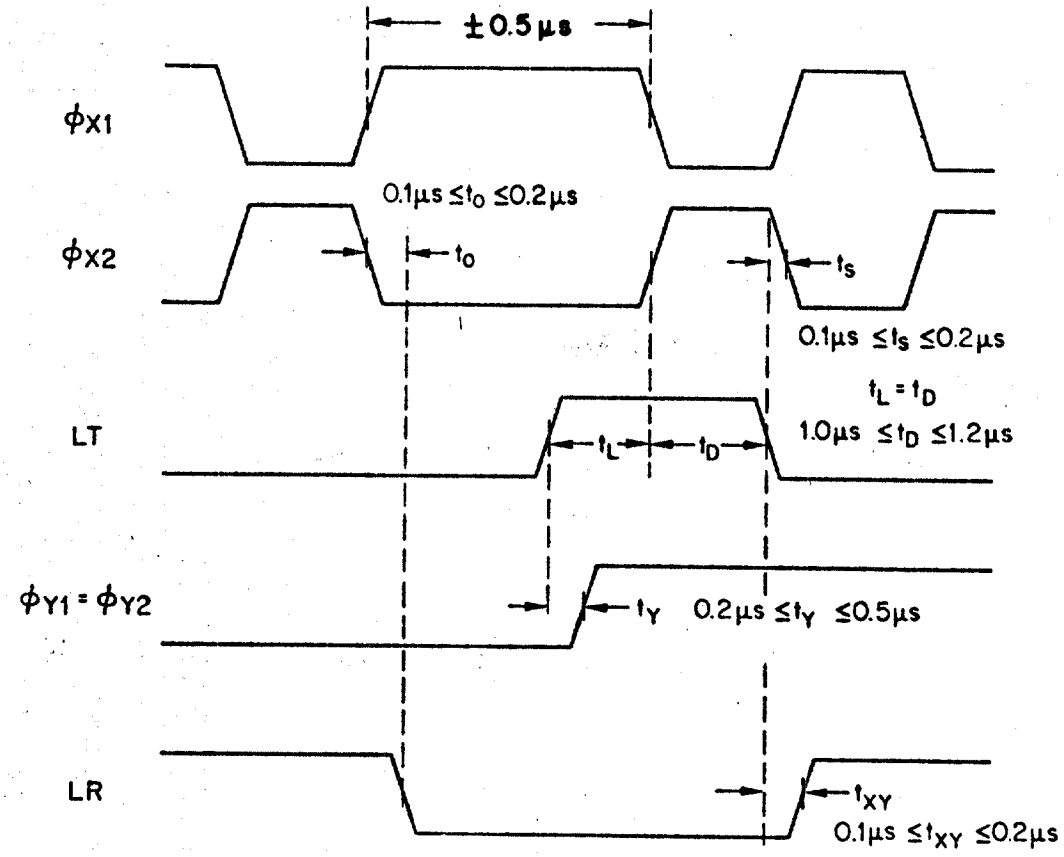

FIGURE 8 - High-Speed Mode Relationships Among X-Clocks and LT and Y-Clocks

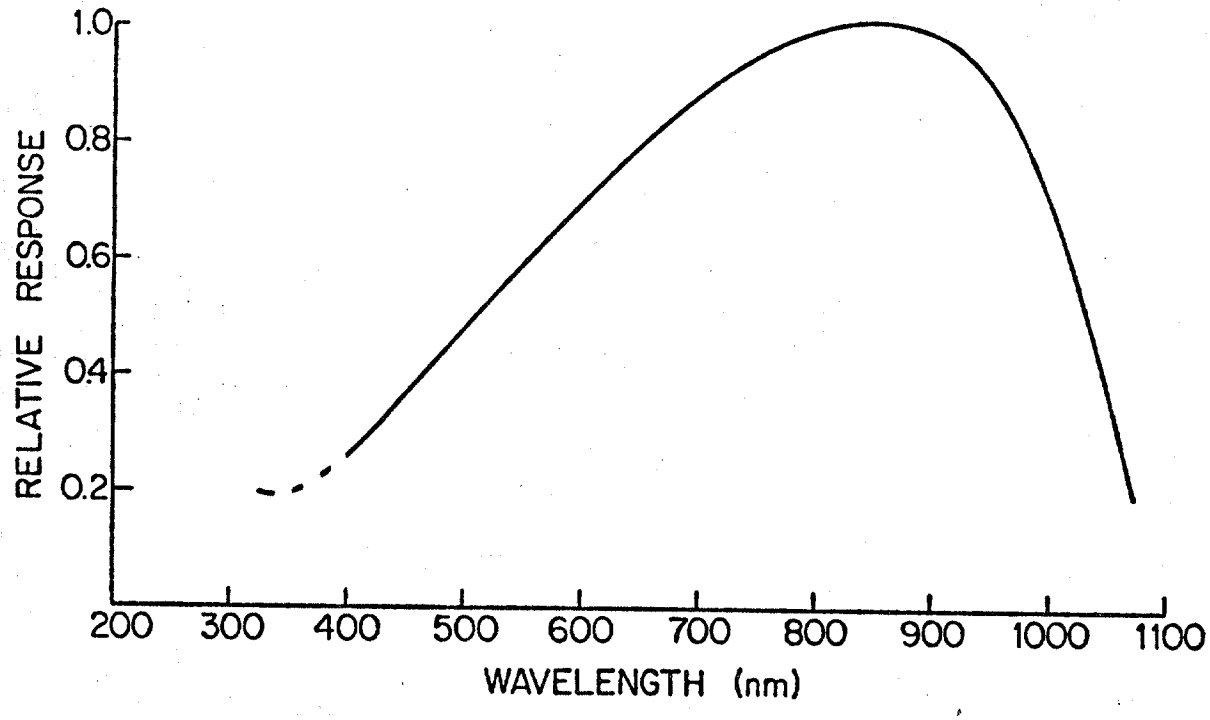

FIGURE 9 - SILICON PHOTODIODE RESPONSE

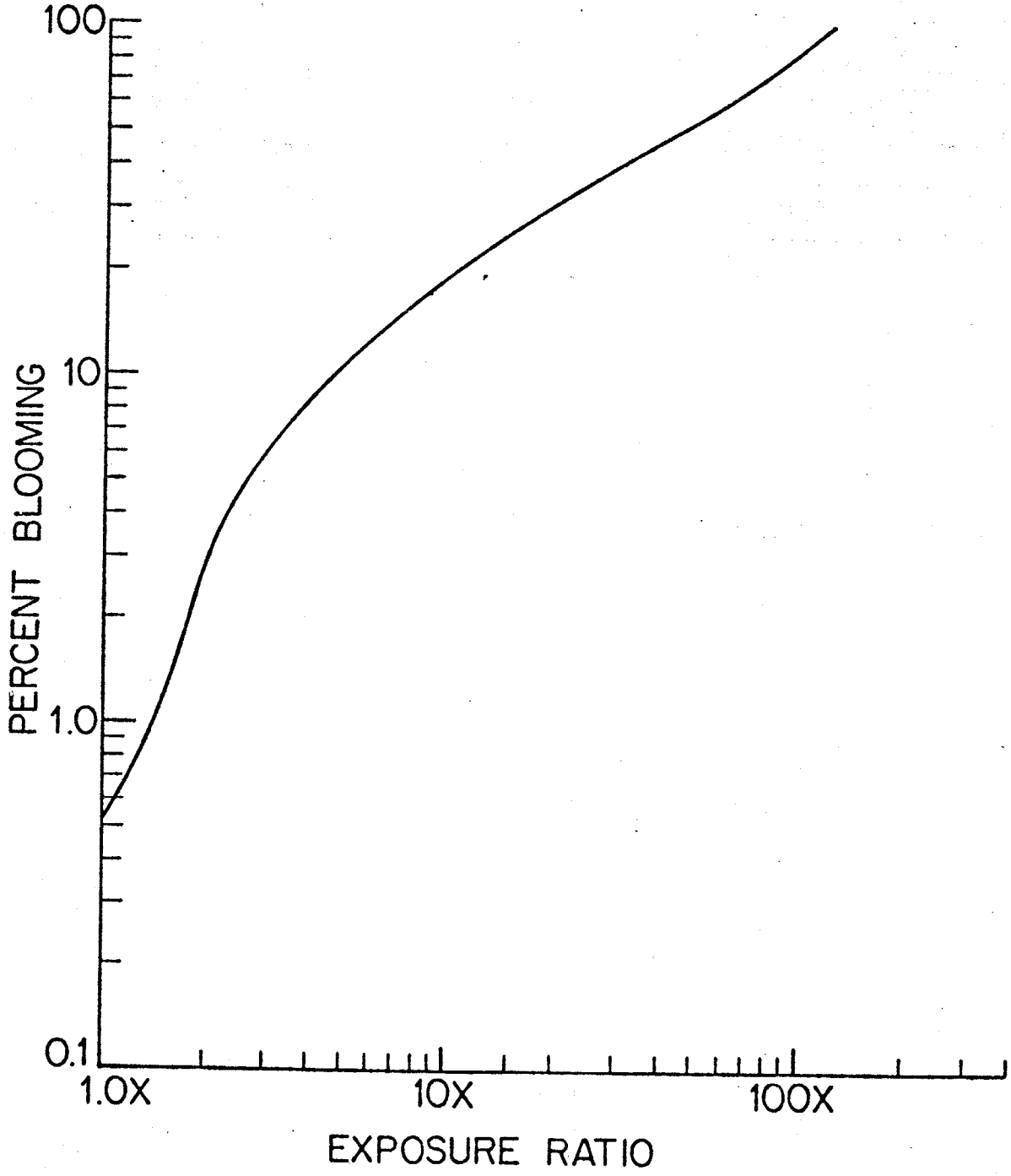

FIGURE 10 - Blooming Ratio (see text under **Optifal to Electrical Performance**)